Multivariate Dynamic Intensity Peaks-Over-Threshold Models *

Nikolaus Hautsch Rodrigo Herrera

Abstract

We propose a multivariate dynamic intensity peaks-over-threshold model to capture extreme events in a multivariate time series of returns. The random occurrence of extreme events exceeding a threshold is modeled based on a multivariate dynamic intensity model allowing for feedback effects between the individual processes. We propose alternative specifications of the multivariate intensity process using autoregressive conditional intensity and Hawkes-type specifications. Likewise, temporal clustering of the size of exceedances is captured by an autoregressive multiplicative error model based on a generalized Pareto distribution. We allow for spillovers between both the intensity processes and the process of marks.

The model is applied to jointly model extreme returns in daily returns of three major stock indices. We find strong empirical support for a temporal clustering of both the occurrence of extremes and the size of exceedances. Moreover, significant feedback effects between both types of processes are observed. Backtesting Value-at-Risk and Expected Shortfall forecasts show that the proposed model does not only produce a good in-sample fit but also reliable out-of-sample predictions. Evidence for a slightly better out-of-sample performance of an autoregressive conditional intensity model compared to a Hawkes specification is provided.

Keywords: Extreme value theory, value at risk, expected shortfall, self-exciting point process, conditional intensity.

JEL classification: C11; C58; C22; F30

1. Introduction

Financial risk management has become an ubiquitous work for banks, companies and financial institutions, especially during the last subprime crisis. The recent global crises has demonstrated

* Nikolaus Hautsch, Department of Statistics and Operations Research, University of Vienna, and Center for Financial Studies, Frankfurt, email: nikolaus.hautsch@univie.ac.at. Rodrigo Herrera, Facultad de Economía y Negocios, Universidad de Talca, email: jrodriherrera@utalca.cl. Hautsch acknowledges research support by the Wiener Wissenschafts-, Forschungs- und Technologiefonds (WWTF).

the importance of modeling and forecasting of extreme events and their dynamic behavior during crisis periods. Classical extreme value theory (EVT) consitutes the mathematical and statistical ground for the description of the distribution of extreme events. Traditional methods to to describe the tail of a loss distribution are the Value-at-Risk (VaR) and the Expected Shortfall (ES), e.g., McNeil & Frey (2000), Cotter & Dowd (2006), Herrera & Schipp (2009), Chavez-Demoulin, Davison & McNeil (2005) or Chavez-Demoulin, Embrechts & Sardy (2014). On the other hand, point process methods allow capturing the dynamic behavior of (extreme) events and are typically applied in the context of portfolio credit risk, market microstructure analysis or jump-diffusion models, see, e.g., Engle & Russell (1998), Russell (1999), Bauwens & Hautsch (2006), Errais, Giesecke & Goldberg (2010), Hautsch (2011). Point process theory moreover provides an elegant formulation of the characterization of the limiting distribution of extreme value distributions[1] and therefore builds a natural complementary framework to extreme value analysis.

In this paper we aim at bringing together both strings of the literature and proposing a dynamic multivariate model capturing the occurrence and size of extremes in a multivariate time series. Important features of the proposed framework are to allow for (i) temporal clustering of both the occurence of extremes and the size thereof, (ii) cross-sectional feedback between individual exceedance intensities and (iii) feedback between the magnitude of exceedances and their intensity. On the one hand, we introduce an autoregressive conditional intensity peaks-over-threshold (ACI-POT) model, which in its most basic form corresponds to the combination of two known models; the ACI model introduced by Russell (1999) and the POT model by Davison & Smith (1990). Moreover, we propose a multivariate extension of a Hawkes-POT model, introduced for the univariate case by Chavez-Demoulin et al. (2005) and recently reviewed in different financial contexts (Chavez-Demoulin & McGill 2012, Herrera 2013).

The major advantage of these new approaches is that they can capture the clustering of extreme events – both over time and the cross-section. Such patterns typically occur in crisis periods and substantially challenge risk management. In addition, this class of processes generates a flexible and computationally tractable multivariate dependence structure, properties that are empirically well documented, Hall, Hautsch & McCulloch (2003),Bauwens & Hautsch (2009),Hall & Hautsch (2007),Bowsher (2007),or Hautsch (2011) and references therein.

[1]The original development of this characterization is due to Pickands (1971) and Smith (1989).

A further contribution, from a purely empirical perspective, is to discuss some stylized facts related to the cluster behavior of extreme events on financial markets. To this end, we consider three well investigated international stock market indexes, the DAX, the S&P 500 and the FTSE 100 index. We show that by means of the multivariate ACI-POT and Hawkes-POT approaches we can well capture these stylized facts and produce reliable forecasts of Value-at-Risk and Expected Shortfall.

The remainder of the paper is organized as follows. In Section 2, we discuss some stylized facts associated to the cluster behavior of extreme events in financial time series. Section 3 summarizes the concepts in EVT from the view point of point process theory. Section 4 introduces the ACI-POT and Hawkes-POT model. In Section 5, we illustrate how to apply the proposed models to produce conditional risk measures, such as the VaR and ES. Section 6 discusses estimation results and diagnostics based on applications of the proposed models to daily returns of international stock indices. Section 7 provides VaR and ES in-sample and out-of-sample backtesting results. Conclusions are given in Section 8.

2. Clustering of Extreme Movements

Clustering of extreme events is recognized as a feature prevailing in most financial time series. The tendency of very large movements of prices (exceedances over a sufficiently high threshold) to be clustered through time is one of the major difficulties to obtain reliable risk measures. A major difficulty is to reliably predict both the size and likelihood of extreme events, e.g., large losses (BCBS (2012)). In this section, we highlight some stylized facts and motivate the need for approaches capturing both dynamic and distributional features of extreme events.

2.1. Clustering of Extreme Gains vs. Extreme Losses

A well-known observation is that co-movements in international stock market returns are asymmetric. In particular, correlations are higher in market downturns than in upturns, and there is a higher level of clustering for losses than for gains. Numerous studies have examined these stylized facts. For instance, Baur, Dimpfl & Jung (2012) find that lower quantiles exhibit positive

dependence in past returns, while upper quantiles display negative dependence for the Dow Jones Stoxx 600 index. Tseng & Li (2011) use different assets and show that larger extreme events tend to cluster more than smaller ones. Similarly, large losses tend to cumulate together more severely than large gains. Relating the high level of clustering for losses and gains, Hamidieh, Stoev & Michailidis (2009) analyze the returns of the S&P 500 index during the period 1960 to 2007 and show that losses exhibit stronger clustering than gains. Olmo (2005) analyze the DAX index over the period 1994-2001 and find a higher level of clustering for large losses than for gains. Jondeau & Rockinger (2003) report evidence of clustering of extremes for a large number of countries, with difference in the cluster size for positive and negative returns, however, not being statistically significant.

To illustrate this stylized fact, we consider an (equal-weighted) portfolio based on the DAX, S&P 500 and FTSE 100 index from 1992 to 2012. A flexible non-parametric tool for capturing different types of extremal dependence is the extremogram introduced by Davis, Mikosch et al. (2009), which can be considered as an analog of the autocorrelation function for extreme events.

The extremogram at lag h is defined by

$$\rho_{AB}(h) = \lim_{x\to\infty} P\left(x^{-1}X_h \in A \mid x^{-1}X_0 \in B\right),$$

for $h = 0, 1, 2, \ldots$, provided the limit exists for two sets A and B bounded away from 0[2]. Similarly, we can define the cross-extremogram

$$\rho_{AB}(h) = \lim_{x,y\to\infty} P\left(y^{-1}Y_h \in A \mid x^{-1}X_0 \in B\right),$$

which can be straightforwardly extended to higher dimensions.

For all (cross-) extremograms displayed in this paper, we utilize a stationary bootstrap to construct confidence intervals with block sizes given by an independent geometric distribution with mean 250, which closely corresponds to the number of yearly trading days. The sampling distributions of the (cross)-extremogram and confidence intervals are obtained based on $10,000$ bootstrap

[2]Normally, in univariate time series the choice of the sets is defined by $A = B = (1, \infty)$, and thus, the extremogram corresponds to the upper tail dependence coefficient between $\mathbf{X}_0$ and $\mathbf{X}_h$.

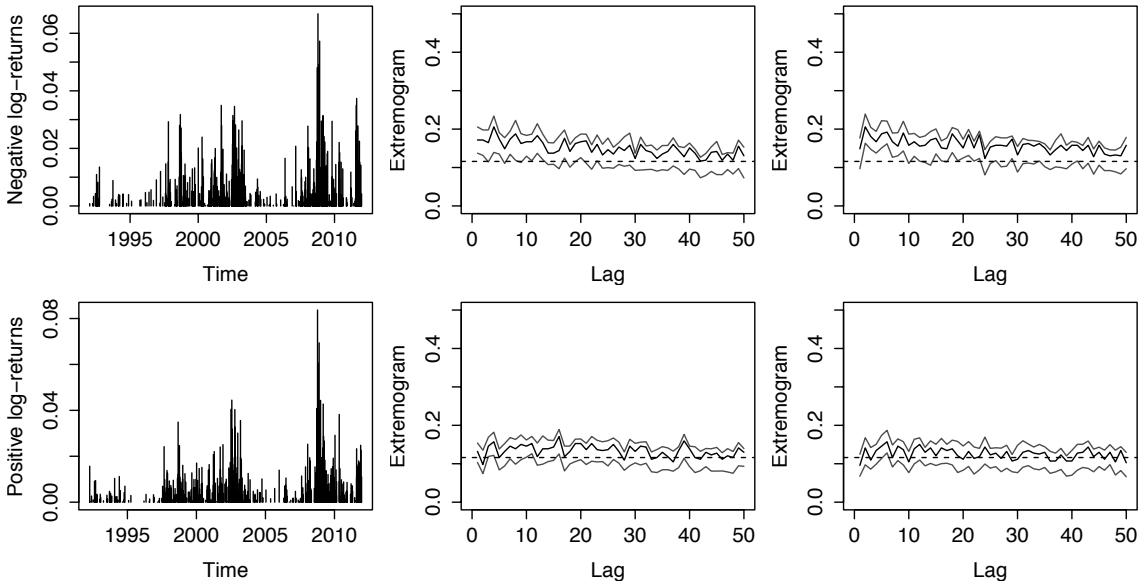

Figure 1: 8.5% of the most extreme losses (top left) and gains (bottom left) for an equal-weighted portfolio based on the DAX, S&P 500 and FTSE 100 index from 1992 to 2012. The sample extremograms are shown in the middle figures with losses in the top and gains in the bottom. The right figures show the cross-extremograms for losses conditional on gains (top right) and gains conditional on losses (bottom right) at different lags. The dashed line corresponds to the value of the extremogram under the null hypothesis of independence at a 95% confidence level obtained by 100 permutations. The sampling distribution of the (cross)-extremogram and confidence intervals are obtained based on 10.000 bootstrap replications.

replications. For a complete discussion and details on the estimation and construction of confidence intervals for extremograms we refer to Davis, Mikosch & Cribben (2012).

Figure 1 displays extremograms and corresponding cross-extremograms. Observe that the (cross-)extremograms decay hyperbolically at the 95% confidence level of independence as lags increase, with losses conditional on gains decaying with slowest rate. In addition, the extremogram of losses and the cross-extremograms for losses conditional on gains show the most significant dependence on many lags. These results are similar to the findings provided by Tseng & Li (2011), Hamidieh et al. (2009) and Olmo (2005).

2.2. Clustering of Extreme Events Across Time

Besides clustering within a time series, we moreover observe a tendency for clusters of extremes occuring simultaneously on different markets. An obvious reason for this observation is an increasing market integration, most distinct in the U.S. and in Europe.

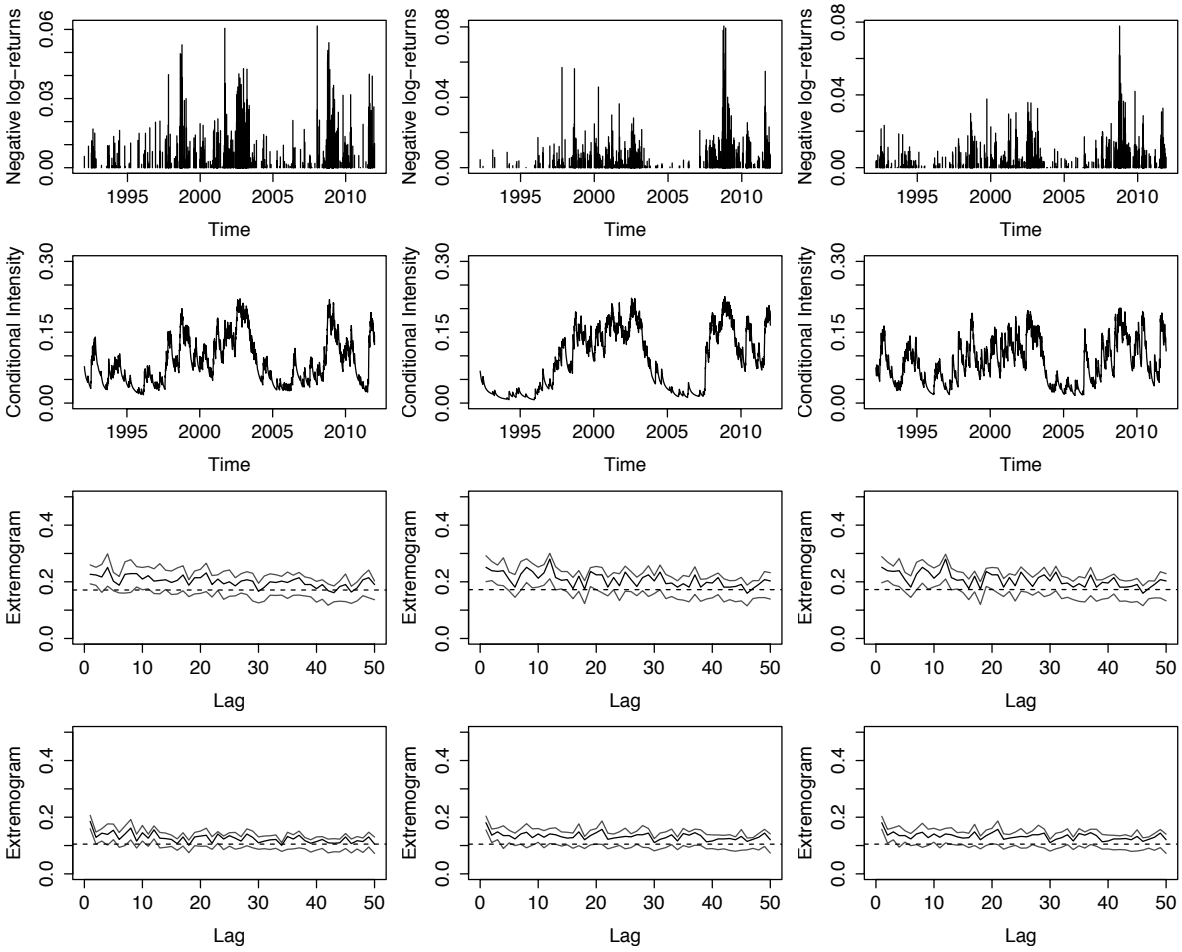

Figure 2: From top to bottom: Time series of 9% of the most extreme losses, the conditional intensity for the occurrence of losses, the trivariate sample cross-extremograms corresponding to $\rho_1(h)$ and $\rho_2(h)$, respectively. From left to right for DAX, S&P 500 and FTSE 100 index.

In Figure 2 we display the time series of 9% of the most negative log returns of the three indices. There seems to be a considerable amount of clustering of extremes across the different stock markets. The first important cluster can be identified during the late 1990s and early 2000s, being associated with the Asian financial crisis in 1997 and the end of the Dot-Com crash in October 2002. The most recent cluster is around the 2008 global financial crisis, starting in 2007 with the Subprime crisis in the US. We moreover, display the trivariate cross-extremograms for the analyzed returns. For instance, let X, Y and Z be the negative log returns of the DAX, S&P 500 and FTSE 100 index, respectively. Then, the third panel corresponds to the cross-extremogram

$$\rho_1(h) = \lim_{x,y,z\to\infty} P\left(y^{-1}Y_h \in A \cup z^{-1}Z_h \in A \mid x^{-1}X_0 \in A\right), \tag{1}$$

with x, y and z being the 0.95 empirical quantiles of the negative log returns and $A = (1, \infty)$. Moreover, in the bottom panel of Figure 2, we display the cross-extremogram

$$\rho_2(h) = \lim_{x,y,z\to\infty} P\left(x^{-1}X_0 \in A \mid y^{-1}Y_h \in A \cup z^{-1}Z_h \in A\right). \tag{2}$$

Interestingly, there is evidence for both types of cross-extremal dependece among the losses, at least for one time lag. Studying the co-clustering of extreme events is of vital importance for the stability of financial systems and implied systemic risk. For instance, Longin & Solnik (2001) show that for the period 1954 to 2003, the top largest daily extreme returns (positive and negative) of the S&P500 index tend to appear around the same date, the stock market crash of October 1987. For a set of European stock markets Poon, Rockinger & Tawn (2004) find that extreme dependence among these countries is much stronger in bear markets than in bull markets, and that some of this dependence is related to volatility co-clustering. Byström (2004) shows that the distance between the fifty most extreme losses for the Swedish index AFF (Affärvärlden's Generalindex) and the Dow Jones Industrial Average index during the period 1980 to 1999 occur within the same month for the half of extremes, while two thirds occur within the same quarter.

The dynamics of such co-clustering of extreme events is readily described by a multivariate intensity. This is what we try to capture by means of the approaches proposed in this paper. To motivate the approach, we display the conditional intensities for the occurrence of extreme events based on a univariate ACI-POT model in the second panel of Figure 2.

2.3. Autocorrelations in Inter-Exceedance Times

The inter-exceedance time is commonly defined as the time interval between consecutive extreme price events. In this vein, times between price events have been used as a proxy for volatility estimation on the basis of price intensities in high frequency data analysis (e.g. Engle 2000, Gerhard & Hautsch 2002).

Classical EVT assumes independent and identically distributed (i.i.d) observations. According to this assumption, the exceedances over a high threshold should behave as a Poisson point process, impliying that inter-exceedance times should be exponentially distributed. Empirical evidence, however, clearly contradicts this assumption, making the direct use of this approach questionable.

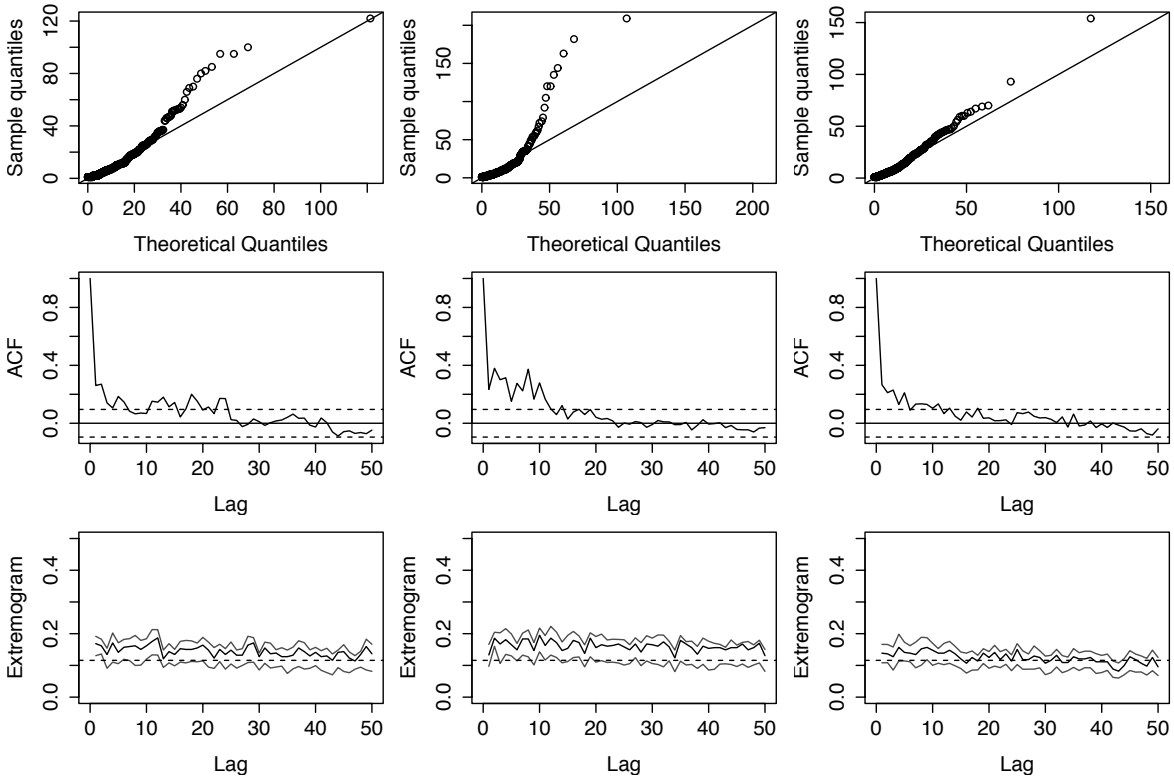

Figure 3: QQ-plots for inter-exceedance times, autocorrelation of inter-exceedance times and sample extremograms for the 9% most extreme losses of DAX, S&P500 and FTSE 100 log returns.

For this reason, a number of new approaches based on the dynamic behavior of inter-exceedance times or the occurrence times of extreme events have been proposed (e.g. Chavez-Demoulin et al. 2005, Chavez-Demoulin & McGill 2012, Herrera 2013).

Figure 3 shows a quantile-quantile plot (top panel) contrasting the empirical distribution of inter-exceedances times to an exponential distribution. In all the cases, the exponential distribution is clearly at odds with empirical observations. Moreover, we report the autocorrelations among inter-exceedance times, providing evidence for a high degree of autocorrelation in all time series. Finally, the bottom panel shows univariate empirical extremograms measuring the impact of a large loss on future realizations on the same stock market. All estimates are highly significant and thus consistent with earlier findings on the presence of serial extremal dependence on stock markets (Chavez-Demoulin & McGill 2012, Davis et al. 2012, Chang, Geman, Hsieh & Hwang 2013).

3. A Point Process Approach to EVT

Consider all negative returns of a given stock market $\{Z_t\}_{t\geq 1}$ and suppose in the moment that all observations are i.i.d and have common distribution function F. If we are interested in the behavior of the maxima of this sequence $M_n = \max\{Z_1, \ldots, Z_n\}$, classical EVT tells us that for given normalizing sequences $a_n > 0$, $b_n \in \mathbb{R}$ and $n \to \infty$, the limiting distribution of the maxima

$$P\left(\frac{M_n - b_n}{a_n} \leq z\right) = F^n\left(a_n z + b_n\right), \tag{3}$$

converges in distribution to the Generalized Extreme Value (GEV) distribution function

$$H_{\xi,\mu,\sigma}(z) = \begin{cases} \exp\left\{-\left(1+\xi\frac{z-\mu}{\sigma}\right)_+^{-1/\xi}\right\}, & \xi \neq 0, \\ \exp\left\{-\exp\left(-\frac{z-\mu}{\sigma}\right)\right\}, & \xi = 0, \end{cases}$$

where μ and $\xi \in \mathbb{R}$, and $\sigma > 0$, corresponding to location, shape and scale parameters, respectively[3]. The convergence in (3) holds if and only if

$$\lim_{n\to\infty} n\left\{1 - F\left(a_n z + b_n\right)\right\} \to -\ln H_{\xi,\mu,\sigma}(z).$$

For these random variables $\{Z_t\}_{t\geq 1}$, we record the time t_j and the magnitude of an extreme event $Y_j = Z_{t_j}$ (the mark), whose size exceeds a given threshold $u > 0$. I.e., we record the pair (t_j, Y_j), in the set $\Omega = (0,1] \times (u, \infty)$ where for convenience the time has been rescaled to the interval $(0,1]$.

According to Pickands (1971), assuming that the losses are i.i.d. and stationary, the two-dimensional point process defined in a sub-region $\mathcal{A} = (0,t] \times (y,\infty)$ by the counting process $N(\mathcal{A}) = \sum_{j\geq 1} \mathbf{1}\{t_j \leq t, Y_j = y\}$ corresponds to a non-homogenous Poisson process with intensity function

$$\lambda(t,y) = \begin{cases} \frac{1}{\sigma}\left(1+\xi\frac{y-\mu}{\sigma}\right)_+^{-1/\xi-1}, & \xi \neq 0, \\ \frac{1}{\sigma}\exp\left(-\frac{y-\mu}{\sigma}\right), & \xi = 0, \end{cases} \tag{4}$$

[3]We define $a_+ = \max(a, 0)$ for any expression of a.

where μ and $\xi \in \mathbb{R}$, and $\sigma > 0$ correspond to the same parameters as in the definition of a GEV distribution function. Consequently, for a set $\mathcal{B} = (t_1, t_2) \times (y, \infty)$, with $\mathcal{B} \subseteq \Omega$, the intensity measure or alternatively the mean of the point process in $\mathcal{B}$ is defined by

$$E\{N(\mathcal{B})\} = \Lambda(\mathcal{B}) = \int_{t_1}^{t_2} \int_{y}^{\infty} \lambda(r, l)\, dr\, dl = -(t_2 - t_1) \ln H_{\xi,\mu,\sigma}(y).$$

A marked point process (MPP) is a stochastic model for the arrival time of events, whose dynamic is characterized by marks associated with other stochastic processes. In our context, the arrival times corresponding to the time whenever a return exceeds a high threshold $u > 0$ is called the ground process, while the marks correspond to the magnitude of losses. Formally, a MPP is defined as the right-continuous counting function $N(t) := N(0, t] = \sum_{j \geq 1} \mathbf{1}\{t_j \leq t,\ Y_j = y\}$ of the time ordered sequence of marked points $\{(t_j, Y_j)\}_{j \geq 1}$ in a defined nonempty countable set $\mathcal{B}$. The internal history or natural filtration of this process is denoted by $\mathcal{H}_t = \{(t_j, Y_j)\ \forall j : t_j < t\}$. According to the definition[4] of a MPP by Daley & Vere-Jones (2003) the intensity of a marked point process can be described as

$$\lambda(t, y \mid \mathcal{H}_t) = \lambda_g(t \mid \mathcal{H}_t)\, g(y \mid \mathcal{H}_t, t), \tag{5}$$

where $\lambda_g(t \mid \mathcal{H}_t)$ corresponds to the intensity of the ground process $N^g(t) = \sum_{j \geq 1} \mathbf{1}\{t_j \leq t\}$ and $g(y \mid \mathcal{H}_t, t)$ to the marks density function, which is conditional on the history of the process and the time t of the last event.

Observe that we can rewrite the intensity of the two-dimensional point process approach described in (4) in terms of a MPP. On the one hand, the ground process corresponds to

$$\lambda_g(t \mid \mathcal{H}_t) = -\ln H_{\xi,\mu,\sigma}(u),$$

[4]Definition 7.3.II in Daley & Vere-Jones (2003).

which is the rate of a Poisson point process of exceedances above the threshold u[5]. On the other hand, the mark density function corresponds to a generalized Pareto density function

$$g_{\xi,\beta}\left(y \mid \mathcal{H}_t, t\right) = \begin{cases} \frac{1}{\beta}\left(1+\xi\frac{y-u}{\beta}\right)_+^{-1/\xi-1}, & \xi \neq 0, \\ \frac{1}{\beta}\exp\left(-\frac{y-u}{\beta}\right), & \xi = 0, \end{cases} \tag{6}$$

where $\beta = \sigma + \xi\left(u-\mu\right)$ is a reparametrized scale parameter. This statistical description is valid In the case of i.i.d. observations, which, however, is empirically not supported. In order to address this problem, we will introduce a more flexible framework allowing for dynamics in the conditional intensity process.

4. Multivariate Intensity Peaks-Over-Threshold Models (MI-POT)

We consider the multidimensional case, i.e., a $M-$variate MPP, $N(t) := \left(N_m(t)\right)_{m=1}^M$, where each dimension $m \in \{1,\ldots,M\}$ is characterized by a double sequence $\left\{\left(t_j^m, Y_j^m\right)\right\}_{j\geq 1}$ of random variables in a set $\mathcal{B}$ defined on some abstract probability space $(\Omega, \mathcal{H}, \mathbb{P})$.

In this framework, t denotes the calendar time (the pooled time) and t_j^m corresponds to the inter-exceedance time with $N_m^g\left(t\right)$ being its marginal ground process. In addition, each m-th component of the MPP is linked to an exceedance Y_j^m constituting the mark. Therefore, the MI-POT is specified via a $M-$variate vector of conditional intensities $\lambda\left(t, y \mid \mathcal{H}_t\right) := \left(\lambda^m\left(t, y \mid \mathcal{H}_t\right)\right)_{m=1}^M$, where $\mathcal{H}_t = \left\{\left(t_j^m, Y_j^m\right) \ \forall\ (m,j) : t_j^m < t,\ m \in \{1,\ldots,M\}\right\}$ denotes the complete internal history.

4.1. The multivariate ACI-POT model

In case of the so-called autoregressive conditional intensity (ACI) POT model, the conditional intensity of the ground process is driven by three main components depending on the history $\mathcal{H}_t$: a left-continuos dynamic process Φ_j that is updated instantaneously after the occurrence of t_{j-1} and does not change until t_j, the last observed excess, $\overline{y}_{j-1}^m = y_{j-1}^m - u$, capturing the influence of the size of extreme events on the conditional intensity by means of the parameter δ_m, and

[5]Observe that this intensity does not depend on time. For this reason, the two-dimensional point process corresponds to a non-homogenous Poisson process.

$\lambda_0^m(t) = \lambda_0^m\left(x(t)\right)$ corresponding to a baseline intensity that changes continuously in terms of its own inter-exceedance times $x^m(t) = t^m - t^m_{N_m^g(t)}$, i.e.,

$$\lambda_g^m\left(t \mid \mathcal{H}_t\right) = \exp\left(\Phi_{N_m^g(t)} + \overline{y}^m_{N_m^g(t)-1}\delta_m\right)\lambda_0^m\left(t\right). \tag{7}$$

As proposed by Russell (1999) we specify the $M\times 1$ vector $\Phi_j := \left(\Phi_j^1, \ldots, \Phi_j^M\right)'$ as a VARMA(1,1) type specification of the form

$$\Phi_{N_m^g(t)} = \left(A^m \varepsilon_{N_m^g(t)-1} + B\Phi_{N_m^g(t)-1}\right) z^m_{N_m^g(t)-1}, \tag{8}$$

where z_j^m denotes an indicator variable that takes on the value one if the j-th event of the pooled process is of type m, and zero otherwise. $A^m = \{a_m\}$ is a $M \times 1$ coefficient vector denoting the impact of the innovation ε_j on the ground intensity of the M-variate processes when the previous extreme event was of type m, and $B = \{b_{mk}\}$ corresponds to a $M \times M$ coefficient matrix of persistence parameters. In addition, the innovation term ε_j is an i.i.d. exponential random vector based on the integrated intensity which is computed by piecewise integration

$$\varepsilon_j := \sum_{m=1}^{M}\left\{1 - \Lambda^m\left(t^m_{j-1}, t^m_j\right)\right\} z_j^m, \tag{9}$$

where $\Lambda^m\left(t^m_{j-1}, t^m_j\right) := \int_{t^m_{j-1}}^{t^m_j} \lambda_g^m\left(s \mid \mathcal{H}_s\right) ds$ is the m-type integrated intensity. This allows the conditional intensity function varying between extreme event arrivals. Finally, the baseline intensity function $\lambda_0^m\left(t\right)$ is specified in form of an appropriate hazard function. In this paper we propose two types of non-monotonous hazard functions. Firstly, the generalized gamma distribution whose hazard function is defined as

$$\lambda_0^m\left(t\right) = \frac{|\nu_m|\left(\nu_m^{-2}\right)^{\nu_m^{-2}}}{\sigma_m x^m(t)\int_{e^{\nu_m\varpi_m - 2\ln\nu_m}}^{\infty} s^{\nu_m^{-2}-1}e^{-s}ds}\exp\left(\nu_m^{-2}\left(\nu_m\varpi_m - \exp\left(\nu_m\varpi_m\right)\right)\right),$$

with $\nu_m \neq 0$, and $\sigma_m, \upsilon_m > 0$. If $\eta_m \sim Gamma(\nu_m^{-2}, 1)$, and $\varpi_m = \ln\left(\nu_m^2 \eta_m\right)/\nu_m$, then $x^m(t) = \exp\left(\upsilon_m + \sigma_m \varpi_m\right)$ follows the generalized gamma distribution (Prentice (1974)). [6] Secondly, we employ the Burr distribution with hazard function given by

$$\lambda_0^m(t) = \frac{\frac{\nu_m \sigma_m}{\upsilon_m}\left(\frac{x^m(t)}{\upsilon_m}\right)^{\sigma_m - 1}}{1 + \left(\frac{x^m(t)}{\upsilon_m}\right)^{\sigma_m}}, \quad \nu_m, \sigma_m, \upsilon_m > 0.$$

These hazard functions are commonly used in the empirical literature since they both exhibit non-monotonic behavior.

On the other hand, a key result in EVT, the Pickands-Balkema-de Haan theorem, demonstrates that the distribution of i.i.d. marks is well approximated by a generalized Pareto distribution (GPD). Similarly to the arrival processes of extremes, however, the magnitudes of exceedances far from being i.i.d. We therefore propose a conditional specification for the mark density, with the size of exceedances following a logarithmic autoregressive conditional process avoiding non-negativity restrictions of the parameters.

Let $\psi^m_{N^g_m(t)} = \ln E\left(\overline{y}^m_{N^g_m(t)} \mid \mathcal{H}_t\right)$ be the log of the conditional expectation of $\overline{y}^m_{N^g_m(t)} = y^m_{N^g_m(t)} - u^m$ and $\varphi^m_{N^g_m(t)} = \psi^m_{N^g_m(t)} - \ln(1-\xi_m)$, where $\xi_m \in \mathbb{R}_+$ is the shape parameter of the GPD. We specify the size of the exceedances for each $m-$component as a multiplicative error model (MEM) (see Engle 2002) given by

$$\begin{aligned}
\overline{y}^m_{N^g_m(t)} &= \exp\left(\varphi^m_{N^g_m(t)}\right)\epsilon^m_{N^g_m(t)} \\
\psi^k_{N^g_m(t)} &= w_m + \rho_m \ln \overline{y}^m_{N^g_m(t)-1} + \beta_m \psi^m_{N^g_m(t)-1} + \gamma_m x^m_{N^g_m(t)-1},
\end{aligned}$$

where ρ_m,β_m, γ_m are parameters, $x^m_{N^g_m(t)-1}$ is the lagged inter-exceedance time, and $\epsilon^m_{N^g_m(t)}$ are i.i.d. generalized Pareto random variables with probability density function given by

$$g_{\xi_m,1}\left(\frac{\overline{y}^m_{N^g_m(t)}}{\exp\left(\varphi^m_{N^g_m(t)}\right)} \mid \mathcal{H}_t, t\right) = \left(1 + \xi_m \overline{y}^m_{N^g_m(t)}\right)^{-1/\xi_m - 1}.$$

[6] This generalized gamma specification is preferred to the original parameterisation by Stacy (1962) since it is more numerically stable near to zero.

The parameter γ_m captures the effect of the most previous elapsed inter-exceedance time on the size of the extreme event. If there is an inverse relationship between the size of the last inter-exceedance time and the size of the exceedances, then γ_m should be negative. This hypothesis is highlighted in recent papers (see Santos & Alves 2012, Santos, Alves & Hammoudeh 2013, Hammoudeh, Santos & Al-Hassan 2013, Herrera & Schipp 2014). In order to ensure the covariance stationarity of $\ln \overline{y}^m_{N^g_m(t)-1}$, $|\rho_m + \beta_m| < 1$ must be satisfied. Under this specification, the conditional density of the exceedance $y^m_{N^g(t)}$ is easily derived as

$$g_{\xi_m,\exp\left(\varphi^m_{N^g_m(t)}\right)}\left(y^m_{N^g_m(t)} \mid \mathcal{H}_t, t\right) = \frac{1}{\exp\left(\varphi^m_{N^g_m(t)}\right)}\left(1+\xi_m\frac{y^m_{N^g_m(t)}-u^m}{\exp\left(\varphi^m_{N^g_m(t)}\right)}\right)^{-1/\xi_m-1}, \quad (10)$$

which corresponds to a generalized Pareto density with time-varying scale parameter $\exp\left(\varphi^m_{N^g_m(t)}\right)$. Replacing the parametrization for the ground process and the marks density function in (5) by the ACI approach (7) and the MEM specification (10) for the marks density, we obtain the multivariate ACI-POT model with the m-th component given by

$$\lambda^m\left(t, y \mid \mathcal{H}_t\right) = \frac{\exp\left(\Phi_{N^g_m(t)} + \overline{y}^m_{N^g_m(t)-1}\delta_m\right)\lambda^m_0\left(t\right)}{\exp(\varphi^m_{N^g_m(t)})}\left(1+\xi_m\frac{y^m_{N^g_m(t)}-u^m}{\exp\left(\varphi^m_{N^g_m(t)}\right)}\right)^{-1/\xi_m-1}. \quad (11)$$

The stationary of the ACI-POT model is ensured if the eigenvalues of the persistence matrix B in (8) lie inside the unit circle, which is equivalent to a spectral radius of the persistence matrix less than one, i.e., $\text{Spr}\left(B\right) = \max\left\{|\varphi| : \det\left(B - \varphi I\right) = 0\right\} < 1$, where φ_i are the eigenvalues of B.

Finally, suppose that we observe the process over the time interval $(0, T]$, the log-likelihood for the ACI-POT model based on the multivariate time series Y is given by

$$\begin{aligned}\ln \mathcal{L}\left(t, y \mid \mathcal{H}_t; \theta_1, \theta_2\right) &= \sum_{m=1}^{M}\sum_{j=1}^{N^g_m(T)} \ln g_{\xi_m,\exp\left(\varphi^m_j\right)}\left(y^m_j \mid \mathcal{H}_t, t; \theta_1\right) \quad (12)\\ &+ \sum_{m=1}^{M}\sum_{j=1}^{N^g_m(T)}\left\{z^m_j \ln \lambda^m_g\left(t_j \mid \mathcal{H}_t; \theta_2\right) - \int_{t^m_{j-1}}^{t^m_j}\lambda^m_g\left(s \mid \mathcal{H}_s; \theta_2\right) ds\right\},\end{aligned}$$

where θ_1, θ_2 and θ_1 denote corresponding parameter sets.

4.2. The Multivariate Hawkes POT Model

The Hawkes process is a self-exciting point process originally introduced by Hawkes (1971). This class of process has wide applications in many different fields, primarily in seismology (Hawkes & Oakes 1974, Ogata 1988) and more recently in finance, e.g., (Bowsher 2007, Dassios, Zhao et al. 2011, Embrechts, Liniger, Lin et al. 2011, Bacry, Dayri & Muzy 2012, Bacry, Delattre, Hoffmann & Muzy 2013). In the context of EVT, an univariate Hawkes POT process was introduced by Chavez-Demoulin et al. (2005) and more recently reviewed in Chavez-Demoulin & McGill (2012).

The ground process for the m-th component is defined in terms of occurrence times of extremes events, i.e.,

$$\lambda_g^m(t \mid \mathcal{H}_t) = \mu_m + \sum_{k=1}^{M} b_{mk} \sum_{j=1}^{N_m^g(t)} h_{mk}\left(t - t_j^k\right). \tag{13}$$

Under this specification, $\mu_m > 0$ corresponds to the immigrant rate or baseline intensity and follows a Poisson process, $h : \mathbb{R} \to \mathbb{R}^+$ is a decay kernel describing the instantaneous influence of the k-th component, and how this deviates from the baseline μ_m through the time. Finally, the parameters $b > 0$ are coefficients defining the $M \times M$ branching matrix $B = \{b_{mk}\}$. Stationarity of the process is ensured if the spectral radius of B being strictly less than 1. In this paper, the decay kernel function is assumed to be exponential

$$h_{mk}\left(t - t_j^k\right) = a_{mk} \exp\left(\delta_m \overline{y}_j^k - a_{mk}\left(t - t_j^k\right)\right),$$

with $a_{mk} > 0$ and $\delta_m \geq 0$.

The influence of the size of extreme events on their intensity is captured by the parameter δ_m. Hence, the ground intensity of the next extreme event depends on the time elapsed since the last event but also on the size of the latter (captured by δ_m).

As in the ACI-POT model, we specify the size of the exceedances for each m-th component based on a MEM model based on a conditional generalized Pareto density function as in (10). Replacing the parametrization for the ground process and the marks density function in (5) by the

Hawkes model defined in (13) and the MEM specification (10) for the marks density, we obtain the multivariate Hawkes-POT model

$$\lambda^m\left(t, y \mid \mathcal{H}_t\right) = \frac{\mu_m + \sum_{k=1}^{M} b_{mk} \sum_{j=1}^{N_m^g(t)} a_{mk} \exp\left(\delta_{mk}\overline{y}_j^k - a_{mk}\left(t - t_j^k\right)\right)}{\exp\left(\varphi_{N_m^g(t)}^m\right)} \left(1 + \xi_m \frac{y_{N_m^g(t)}^m - u^m}{\exp\left(\varphi_{N_m^g(t)}^m\right)}\right)^{-1/\xi_m - 1}. \tag{14}$$

The log-likelihood is then given by

$$\begin{aligned} \ln \mathcal{L}\left(t, y \mid \mathcal{H}_t; \theta_1, \theta_2\right) &= \sum_{m=1}^{M} \sum_{j=1}^{N_m^g(T)} \ln g^m_{\xi_m, \exp\left(\varphi_j^m\right)}\left(y_j^m \mid \mathcal{H}_t, t; \theta_1\right) \\ &\quad + \sum_{m=1}^{M} \left\{ \sum_{j=1}^{N_m^g(T)} \ln \lambda_g^m\left(t_j \mid \mathcal{H}_t; \theta_2\right) - \int_0^T \lambda_g^m\left(s \mid \mathcal{H}_s; \theta_2\right) ds \right\}, \end{aligned}$$

where θ_1, θ_2 and θ_1 denote corresponding parameter sets.

Note that the parameters associated with the two models for intensities and marks are disjoint which allows us to estimate them separately.

5. Improving conditional risk measures

The Basel Committee on Banking Supervision has proposed using ES instead of VaR as an internal model-based approach for regulatory market risk capital, mainly because of the inability of VaR to capture tail risk (see BCBS 2012, BCBS 2013). However, Gneiting (2011) demonstrate that, though ES is a coherent risk measure (Artzner, Delbaen, Eber & Heath 1999) and is able to capture tail risk, it does not satisfy the requirement of elicitability. I.e., it cannot be straightforwardly backtested. The virtues and limitations of both risk measures have forced regulators and practitioners to adopt one of them, and therefore, the features of coherence or elicitability. In this paper, we show the derivation of both risk measures based on the proposed MI-POT model.

Let us consider all losses $\{Y_t\}_{t\geq 1}$ with cumulative distribution function F. For ease of exposition, we omit the superscript m. ES is estimated by firstly obtaining the VaR at confidence level α,

which is equivalent to estimating the predictive distribution ($F_{Y_{t+1}|\mathcal{H}_t}\left(y_\alpha^{t+1}\right)$) for the returns over the next period

$$y_\alpha^{t+1} = F^{-1}_{Y_{t+1}|\mathcal{H}_t}(\alpha) := VaR_\alpha^{t+1}.$$

We compute $1 - F_{Y_{t+1}|\mathcal{H}_t}(y)$ as

$$\begin{aligned}\overline{F}_{Y_{t+1}|\mathcal{H}_t}(y) &= P(Y_{t+1} > y \mid \mathcal{H}_t) \\ &= P(Y_{t+1} > u \mid \mathcal{H}_t)\, P(Y_{t+1} > y + u \mid Y_{t+1} > u, \mathcal{H}_t).\end{aligned}$$

The probability $P(Y_{it+1} > u \mid \mathcal{H}_t)$ can be calculated as

$$\begin{aligned}P(N_g(t+1) - N_g(t) > 0 \mid \mathcal{H}_t) &= 1 - \exp\left(-\int_t^{t+1} \lambda_g(s \mid \mathcal{H}_s)\, ds\right), \\ &\approx \lambda_g(t \mid \mathcal{H}_t),\end{aligned}$$

where the last result is obtained by using the asymptotic identity $\ln(x) \approx x - 1$ as $x \to 1$. The conditional probability of exceedances is computed as

$$\begin{aligned}P(Y_{t+1} > y + u \mid Y_{t+1} > u, \mathcal{H}_t) &= \frac{\int_t^{t+1}\int_{y+u}^{\infty} \lambda(s, l \mid \mathcal{H}_s)\, dsdl}{\int_t^{t+1}\int_u^{\infty} \lambda(s, l \mid \mathcal{H}_s)\, dsdl} \\ &= 1 - \left(1 + \xi\frac{y-u}{\exp\left(\varphi_{N^g(t)}\right)}\right)^{-1/\xi} := \overline{G}_{\xi,\exp\left(\varphi_{N^g(t)}\right)}(y \mid \mathcal{H}_t, t),\end{aligned}$$

where $\overline{G}_{\xi,\exp\left(\varphi_{N^g(t)}\right)}$ denotes the conditional generalized Pareto distribution survival function. Finally, the VaR is defined in terms of the quantile y_α^{t+1} with $P\left(Y_{t+1} > y_\alpha^{t+1} \mid \mathcal{H}_t\right) = 1 - \alpha$. implying

$$VaR_\alpha^{t+1} = u + \frac{\exp\left(\varphi_{N^g(t)}\right)}{\xi}\left\{\left(\frac{1-\alpha}{\lambda_g(t \mid \mathcal{H}_t)}\right)^{-\xi} - 1\right\}.$$

From this result, the associated conditional ES is calculated by observing that the conditional distribution of extreme events above the VaR given the history $\mathcal{H}_t$ is

$$ES_{\alpha}^{t+1} = \frac{1}{1-\alpha}\int_{\alpha}^{1} VaR_{s}^{t+1} ds = \frac{VaR_{\alpha}^{t+1}}{1-\xi} + \frac{\exp\left(\varphi_{N^g(t)}\right) - \xi u}{1-\xi}. \tag{15}$$

Finally, observe that

$$\lim_{\alpha \to 1} \frac{ES_{\alpha}^{t+1}}{VaR_{\alpha}^{t+1}} = \frac{1}{1-\xi}, \tag{16}$$

with the limit not depending on time.

Recently, the Basel Committee citeBasel2013 proposes to replace the VaR at the 0.99 confidence level in internal model-based approaches with ES evaluated at 0.975 confidence level. According to the Basel Committee, ES is less sensitivity to extreme events, and therefore, should account for the tail risk in a more comprehensive form. We analyze this proposition in the next section.

6. Applications

6.1. Empirical Setting

We employ DAX, S&P 500 and FTSE 100 index log returns through the sample period from January 2, 1992 to December 31, 2012 covering 4,884 trading days. The first application is based on a bivariate model for the analysis of the clustering of extreme losses and gains of an equally-weighted portfolio based on these indexes. The second application considers a trivariate model to jointly model negative log-returns of the three indexes.

To determine the tail threshold u, we follow the statistic proposed by Reiss & Thomas (2007) to determine the number of exceedances k by

$$\arg\min_{k} f(k) = \frac{1}{k}\sum_{i=1}^{k} i^{\beta} \left| \hat{\xi}_i - \text{median}\left(\hat{\xi}_1, \ldots, \hat{\xi}_k\right) \right|,$$

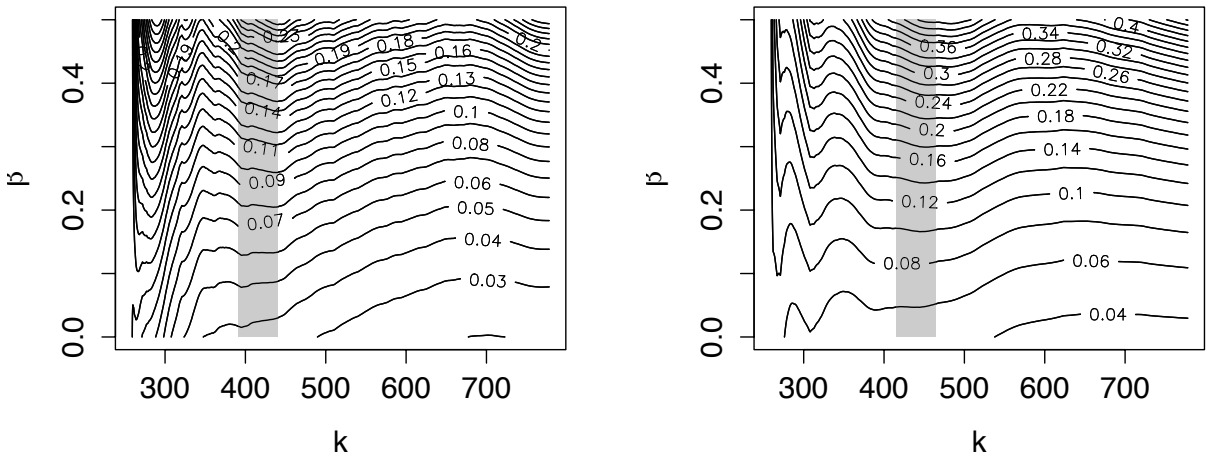

Figure 4: Results for the threshold selection for the bivariate application. The left panel shows the results of the statistic for losses, while the rigth panel displays the results for gains of the portfolio. The gray rectangle shows the subset that seems to be more stable for the shape parameter (x-axis) for different tuning parameters β (y-axis).

where $\hat{\xi}_i$ is the estimate of the shape parameter for the sample fraction of extremes above upper order statistic i, and $\beta \in [0, 0.5]$ is a tuning parameter. The idea is to find that sample proportion for which the distribution of the shape parameters is stable. Figure 4 displays the corresponding results. We observe that a proportion between 395 and 445 observations for gains and losses seems to be a satisfactory size. We choose working with 420 observations, corresponding to 8.5% of the most extreme events for losses and gains. For the trivariate case, we determine a threshold of 9% as a reasonable choice.

6.2. Empirical results

Modeling Extreme Gains and Losses

Table 1 in the Appendix displays the estimation results for both the ACI-POT and Hawkes-POT specification. In Figure 5, we plot the corresponding estimates of the conditional intensity of the ground processes of positive and negative log returns, respectively, based on both the Hawkes-POT and ACI-POT model with generalized gamma and Burr baseline function, respectively. The bottom panel shows a barcode plot, where the bars color in black or gray indicate those log returns that cause extreme observations.

The best fit is achieved for an ACI-POT model with generalized gamma baseline function, though the difference to a specification based on a Burr baseline function is small. For both ACI-POT models, we find evidence for spill-over effects between positive and negative extreme observations, as captured by the persistence matrix B. Note that the persistent coefficient associated with negative extreme events ($b_{22} = 0.652$) is larger than that for positive extreme events ($b_{11} = 0.499$), which indicates that the extent of clustering of extremes tends to be larger for extreme losses. Moreover, the off-diagonal persistence coefficients reveal that negative extreme events cause more frequently positive extreme events than vice versa ($b_{21} > b_{12}$). Finally, for the ACI-POT models, we also find evidence for spill-overs in the innovations, as reflected by large a_m coefficients.

Similarly, the estimates of the Hawkes-POT model reveal evidence for spill-over effects between negative and positive returns and a clustering of extreme events. The estimated persistence matrix B indicates that negative extreme events are more likely to be followed by another negative event ($b_{22} = 0.547$) than by a positive extreme event ($b_{12} = 0.537$).

Overall, our estimates strongly support an obvious asymmetry between positive and negative extreme returns, as discussed in Section 2. This is in line with the the overreaction hypothesis in behavioral finance (Bondt & Thaler (1985), Bondt & Thaler (1987)), predicting that negative extreme observations in stock prices yield positive extreme returns to correct the overreaction of the market. We moreover find strong evidence for the conditional intensity of the ground process in both MI-POT approaches exhibiting a marked cross-sectional interdependence. This result is consistent with several previous studies (, Longin & Solnik 2001, Poon et al. 2004, Byström 2004) which emphasize this cross-effect.

The estimates of the MEM specification for the magnitude of marks provide clear evidence for a clustering of the size of exceedances. Hence, small (large) exceedances are likely to be followed by small (large) exceedances. The coefficients γ_m, moreover, are both negative and strongly significant, indicating that long lagged inter-exceedance times imply a reduction of the expected size of marks. This is in agreement with the hypothesis put forward by Santos & Alves (2012).

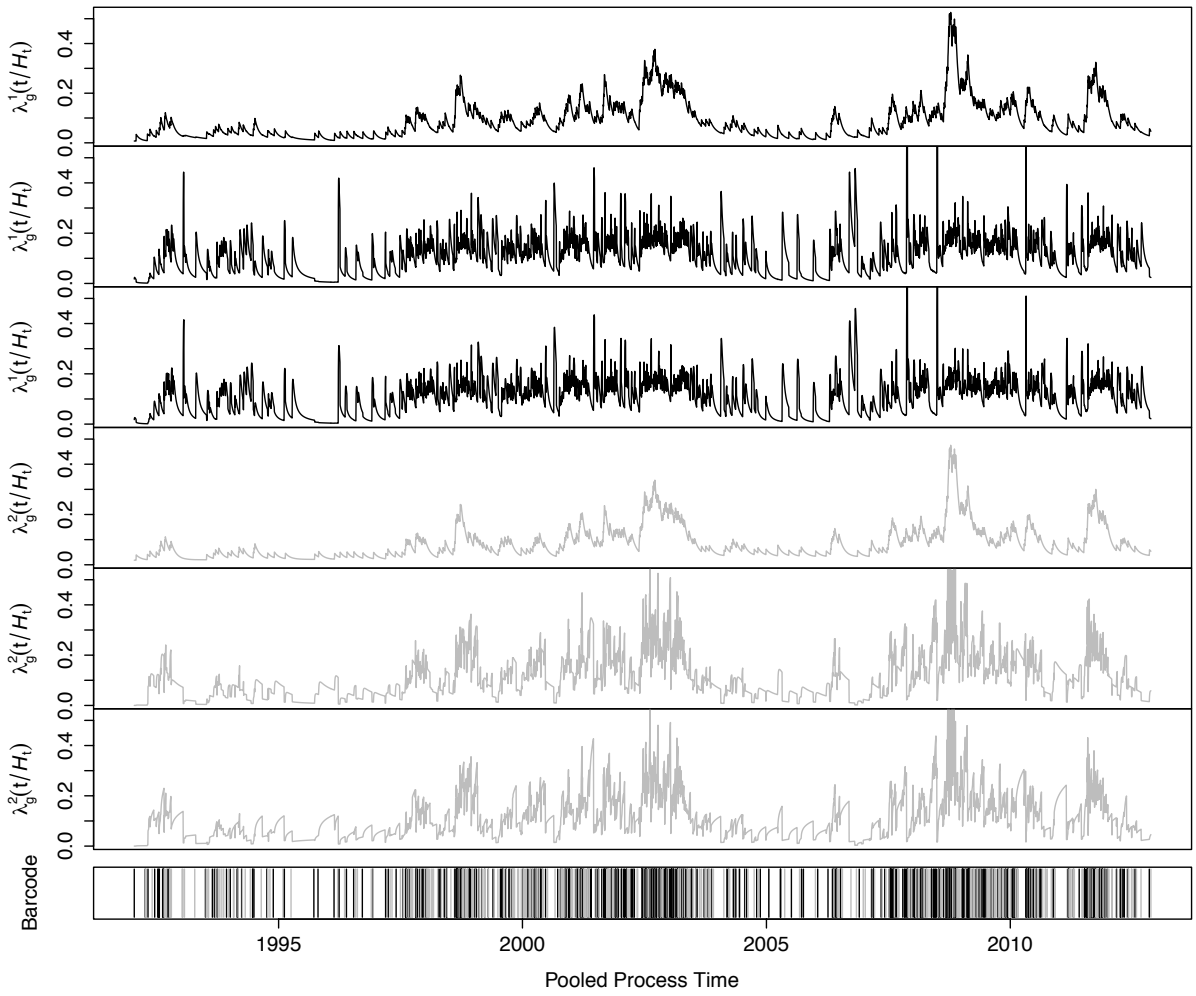

Figure 5: Bivariate conditional intensity of the ground process for the analyzed index portfolio. The first three panels from top to down show the estimated conditional intensity of the ground processes for positive log-returns, while the following three panels exhibit the conditional intensity of the ground processes for negative log-returns. The underlying models are the Hawkes-POT and ACI-POT specification with a generalized gamma and Burr baseline function, respectively. The bottom panel displays a barcode plot, where the black or gray colors indicate the log returns causing the extreme observation.

Residual diagnostic tests for the MI-POT approach are based on the de-meaned integrated intensities of the ground process ($\varepsilon_j = 1 - \int_{t_{j-1}^m}^{t_j^m} \lambda_g^m \left(s \mid \mathcal{H}_s\right) ds$), which, according to the random change theorem, should be i.i.d. standard exponentially distributed with mean zero. Accordingly, the test for excess dispersion of Engle & Russell (1998) is $\sqrt{n_\varepsilon/8}\tilde{\sigma}_\varepsilon^2$, where n_ε corresponds to the number of residuals and $\tilde{\sigma}_\varepsilon$ is the empirical standard deviation of the residuals series. Under correct model specification, the test test statistic is asymptotically normally distributed.

We observe that the residuals are on average close to zero, with standard deviations being not far from unity. Moreover, according to Ljung-Box statistics, the assumption of independence cannot be rejected indicating that the model is able to capture the dynamics in the data pretty well. The test on excess dispersion, however, reveals slight evidence for overdispersion, indicating that both approaches are still not sufficiently flexible to capture the distributional properties of inter-exceedance times.

Modeling Cross-Sectional Spillovers in Extremes

Table 2 gives the estimation results based on trivariate MI-POT models for extremes in DAX, S&P500 and FTSE100 returns. The best-fitting specification is the ACI-POT model with generalized gamma baseline function. It turns out that the flexible parametrization of the ground process in the ACI-POT specification compared to the Hawkes-POT specification significantly improves the explanatory power.

In case of the ACI-POT models, the ground process is pretty persistent with relatively low innovations coefficients and pretty high persistence parameters. All persistence parameters are significant and support stationarity of the underlying process. In both ACI-POT models, the baseline functions show a non-monotonic shape of bathtub or inverted U-shaped form. We moreover find the influence of the exceedance size on the conditional intensity of the ground process, captured by the coefficient δ_m, being significant in both ACI-POT specifications. Hence, extreme events in one series increase the conditional intensity for the next extreme event in the same series, but also in the other series. This result is in line with the estimates of the trivariate sample extremograms in Figure (2) and with previous studies of extreme dependence in international stock markets (Poon,

Rockinger & Tawn (2003), Baltzer, Cappiello, Santis & Manganelli (2008), Herrera & Eichler (2011)).

The estimates of the Hawkes-POT model support these findings. The flexibility of the Hawkes-POT model allows us, moreover, to capture even the influence of the size of each loss on the intensity of each ground process. In the dynamic specification for the marks we find a strong persistence with coefficients $\beta_m < 1$. Hence, exceedance sizes are clearly autocorrelated and, moreover, depend negatively on the length of past inter-exceedance waiting times, as reflected by the coefficient γ_m.

As in the bivariate model above, residual diagnostics reveal that both MI-POT specifications capture the distributional and dynamic features in the underlying series sufficiently well.

7. MI-POT Based VaR and ES Forecasting

7.1. Backtesting

To assess the predictive performance of MI-POT models, we evaluate the accuracy of the VaR, first, in-sample, and then in terms of out-of-sample backtesting procedures. To this end, we utilize a battery of tests proposed in the literature, which are described in details in Herrera & Schipp (2013). The first three test are based on a Markov chain type model with two states as introduced in Christoffersen (1998), corresponding to an unconditional coverage test (LR_{uc}), a test of independence of failures (LR_{ind}) and a conditional coverage test (LR_{cc}), which is a combination of the last two tests. Moreover, we implement the dynamic quantile tests proposed by Engle & Manganelli (2004) building on linear regression settings. The first is the dynamic quantile hit (DQ_{hit}) test, where the regressors are the lagged de-meaned hits of failures, while the dynamic quantile VaR (DQ_{VaR}) test uses in addition contemporaneous VaR estimates. Finally, we employ the measure V^{ES} evaluating the difference between the predicted ES ($\hat{ES}_\alpha^t$) and the observed return (R_t) at time t, given that this return has exceeded the actual VaR, i.e.,

$$V^{ES} = \frac{\sum_{t=0}^{T} \left(R_t - (-\hat{ES}_\alpha^t) \right) \mathbf{1}_{\left\{ R_t < -\hat{VaR}_\alpha^{t+1} \right\}}}{\sum_{t=0}^{T} \mathbf{1}_{\left\{ R_t < -\hat{VaR}_\alpha^{t+1} \right\}}}.$$

This statistic is close to zero if the model is appropriate (Embrechts, Kaufmann & Patie (2005)). However, its weakness is that it depends on the accuracy of the VaR estimates, since only returns below the VaR are taken into account.

Emmer, Kratz & Tasche (2013) propose a framework to backtest ES based on a representation in terms of integrated VaRs

$$\begin{aligned} ES_{\alpha}^{t+1} &= \frac{1}{1-\alpha}\int_{\alpha}^{1} VaR_{s}^{t+1}ds \\ &\approx \frac{1}{4}\left[VaR_{\alpha}^{t+1} + VaR_{0.75\alpha+0.25}^{t+1} + VaR_{0.5\alpha+0.5}^{t+1} + VaR_{0.25\alpha+0.75}^{t+1}\right]. \end{aligned} \tag{17}$$

This allows making use of backtesting techniques developed for VaR and as described above.

Accuracy of MI-POT Based Risk Forecasts

To assess the accuracy of both approaches to estimate and predict the VaR and ES at different confidence levels, we adopt the following procedure: The parameters of the three models are estimated using the sample from January 2, 1992 to December 31, 2012. The parameters of the models are then used to compute one-day-ahead forecasts of the 99%-VaR and 97.5%- ES in the forecast period January 2, 2013 to December 31, 2013.[7] Note that the model parameters are not re-estimated each trading day since the additional information obtained from the forecast sample is negligible compared to the sample period data and results would only change very mildly.

Table 3 gives the test outcomes for the VaR and ES estimations in-sample and out-sample for the trivariate MI-POT models jointly modeling extremes in all three index series. Note that we need to estimate the VaR confidence levels $(0.975, 0.98125, 0.9875, 0.99375)$ in order to make use of the integral representation (17) allowing to backtest the ES at the 97.5% level. For comparison purposes we also report the VaR at 0.99 level for comparison purposes.

According to the test outcomes, the specification providing the most accurate in-sample fit is the Hawkes-POT model. A slightly worse performance is observed for the ACI-POT models indicating some evidence for a minor over-estimation of risk at this confidence level. These findings

[7] The Basel Committee (see BCBS (2013)) recommends changing the risk-based capital framework building on 99%-VaR to 97.5%-ES. These confidence levels are used in our empirical analysis.

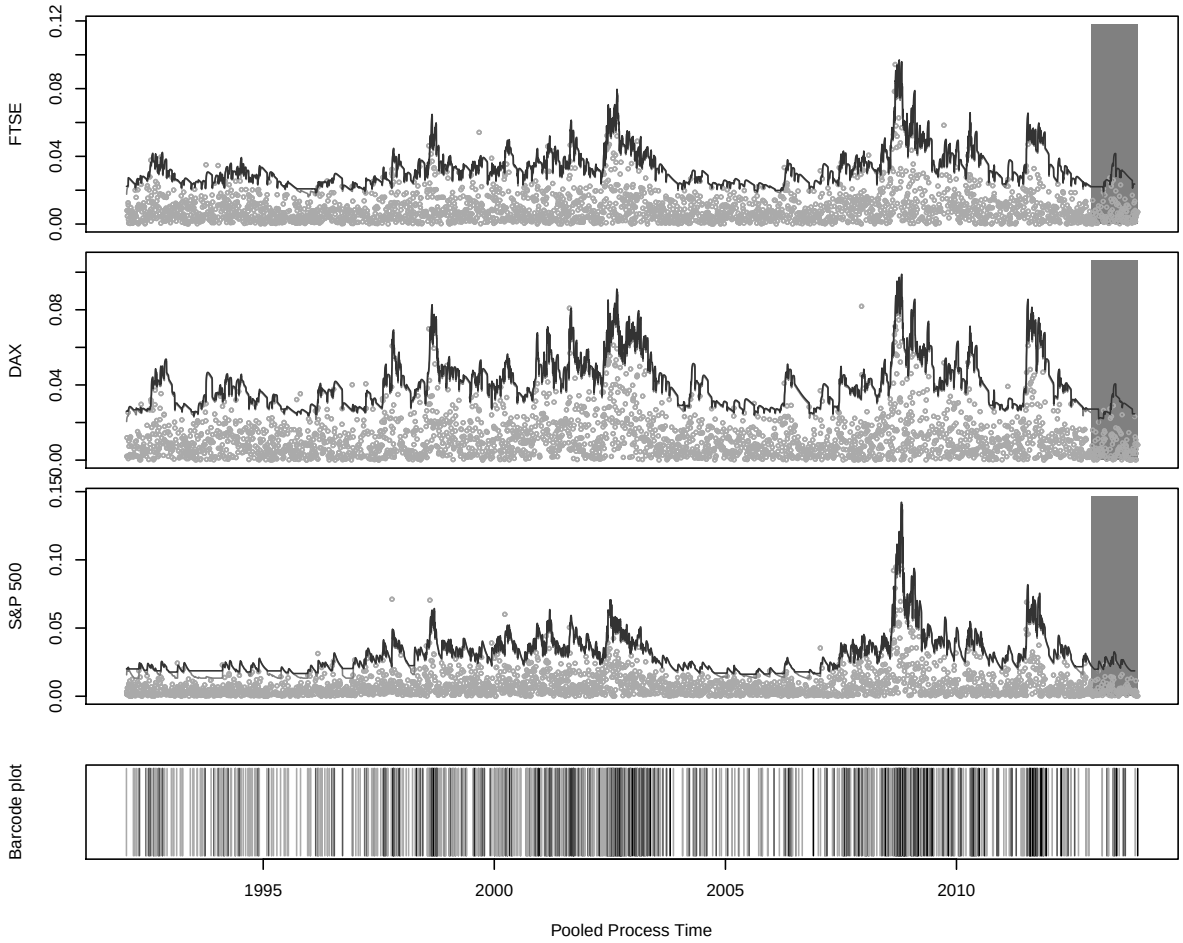

Figure 6: From top to bottom: estimated 99%-VaR (gray line) and 97.5% ES (black line) for the trivariate ACI-POT model with Burr hazard function, applied to negative log returns of the FTSE 100, DAX and S&P 500 indexes. In-sample period: January 2, 1992 to December 31, 2012. Out-of-sample period: January 2, 2013 to December 31, 2013 (marked by dark background). The bottom panel shows a barcode plot with light colors indicating extreme events in the FTSE 100, DAX, or S&P 500 and the the middle dark colors indicating a simultaneous extreme event in any pair of negative log returns. The dark black color marks a simultaneous extreme event in all three negative log return series.

are supported by the statistic V^{ES}, revealing the best performance for the Hawkes-POT model (with a mean of $V^{ES} = 1.09 \times 10^{-4}$) for the chosen confidence level. The ACI-POT models performs marginally weaker (with $V^{ES} = 1.17 \times 10^{-4}$ and $V^{ES} = 1.20 \times 10^{-4}$ for the ACI-POT model with generalized gamma and Burr baselines, respectively).

Figures 6, 7 and 8 display the estimated VaR and ES times series based on the two types of ACI-POT specifications (using a Burr and generalized gamma baseline function, respectively) and the Hawkes-POT model, respectively. The figures also show barcodes visualizing to which extent extremes occur individually or jointly in the three series. We observe the highest estimates of VaR and ES in all series during the years 2000-2002. During this period, the three stock market indices experienced large losses due mainly to the Dot-Com crash, and the aftermath of 9/11 terrorist attacks. After this period, the level of extreme risks declined until the subprime crisis in 2007 followed by the global crisis in 2008/9. We note that most of the extreme events do not occur exactly on the same day[8]. In fact, only the S&P 500 losses exhibit simultaneities with extreme events in other return series on the same day. Specifically, 169 of 441 losses occur simultaneously with the DAX and 14 of 441 losses with the FTSE100. Only one extreme event happens simultaneously in DAX and FTSE100 returns, and only one extreme event occurs simultaneously on all three stock markets.

The backtesting results displayed in Table 3 indicate a quite good performance of both types of MI-POT models. Based on the ACI-POT models most of the confidence levels are correctly estimated. Based on the Hawkes-POT approach, however, two of the VaR confidence levels for DAX returns are overestimated. These results suggest that Hawkes-POT models might have the tendency to overfit in-sample but slightly underperform out-of-sample. Therefore, working with ACI-POT models is slightly preferable in a backtesting context. In fact, the Hawkes-POT model tends to give estimates for the VaR and ES slightly larger than the ACI-POT models, which is also reflected in the measure V^{ES}.

Finally, we analyze the difference between the predicted 99%-VaR and 97.5%-ES based on both approaches. From a theoretical point of view, the ratio between both measures should be close to $\overline{ES}_{0.975}/\overline{VaR}_{0.99} \approx 0.4^{\xi}/(1-\xi)$ [9]. Since for all return series analyzed $\xi > 0$, the ratio

[8] For the DAX, S&P500 and FTSE100 we observe 269, 257 and 425 extreme events, respectively

[9] Observe that $\frac{\overline{VaR}_{0.975}}{\overline{VaR}_{0.99}} \approx 0.4^{\xi}$ and from 16 we know that $\frac{\overline{ES}_{0.975}}{\overline{VaR}_{0.975}} \approx \frac{1}{1-\xi}$.

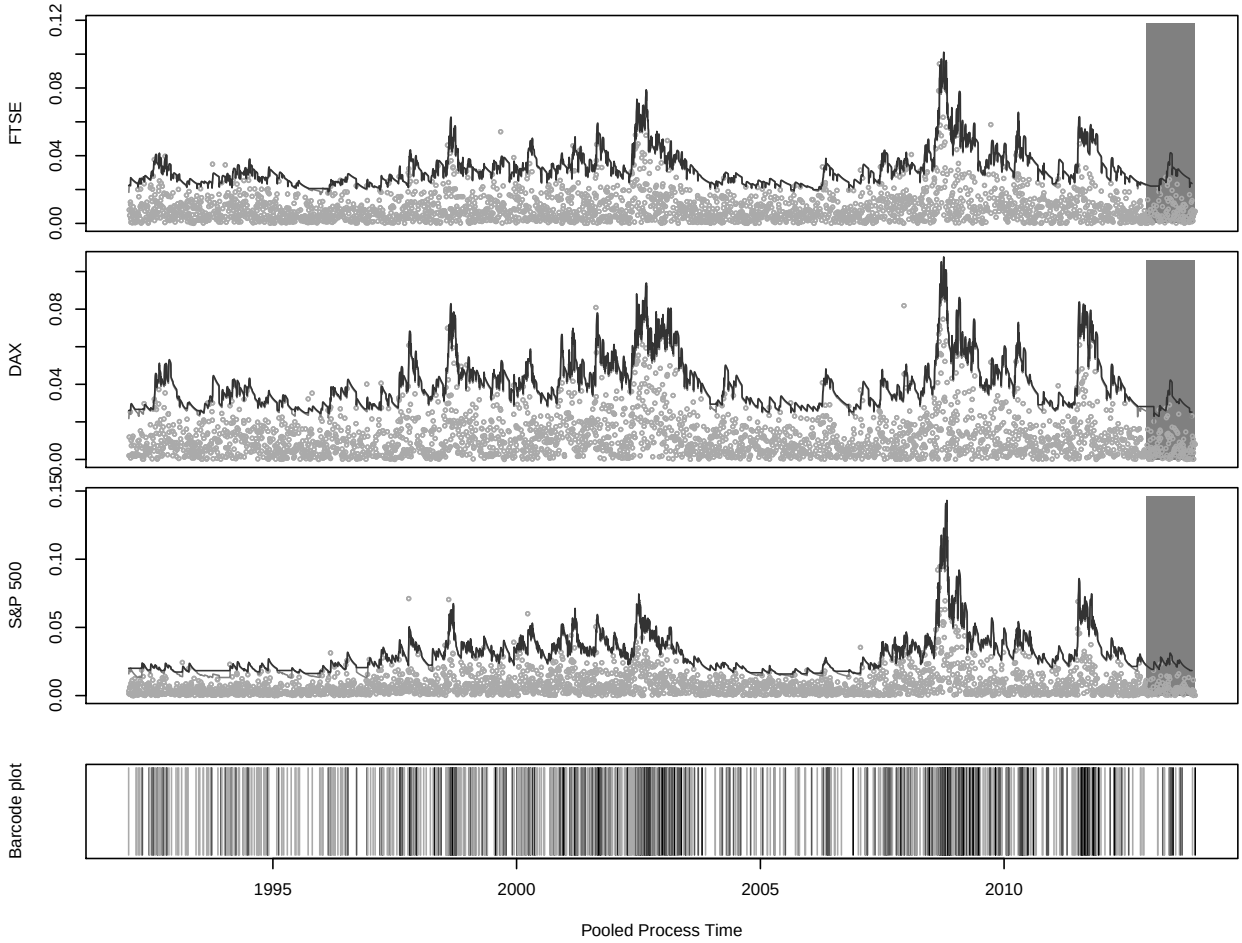

Figure 7: From top to bottom: estimated 99%-VaR (gray line) and 97.5% ES (black line) for the trivariate ACI-POT model with generalized gamma hazard function, applied to the negative log returns of the FTSE 100, DAX and S&P 500 indexes. In-sample period: January 2, 1992 to December 31, 2012. Out-of-sample period: January 2, 2013 to December 31, 2013 (marked by dark background). The bottom panel shows a barcode plot with light colors indicating extreme events in the FTSE 100, DAX, or S&P 500 and the the middle dark colors indicating a simultaneous extreme event in any pair of negative log returns. The dark black color marks a simultaneous extreme event in all three negative log return series.

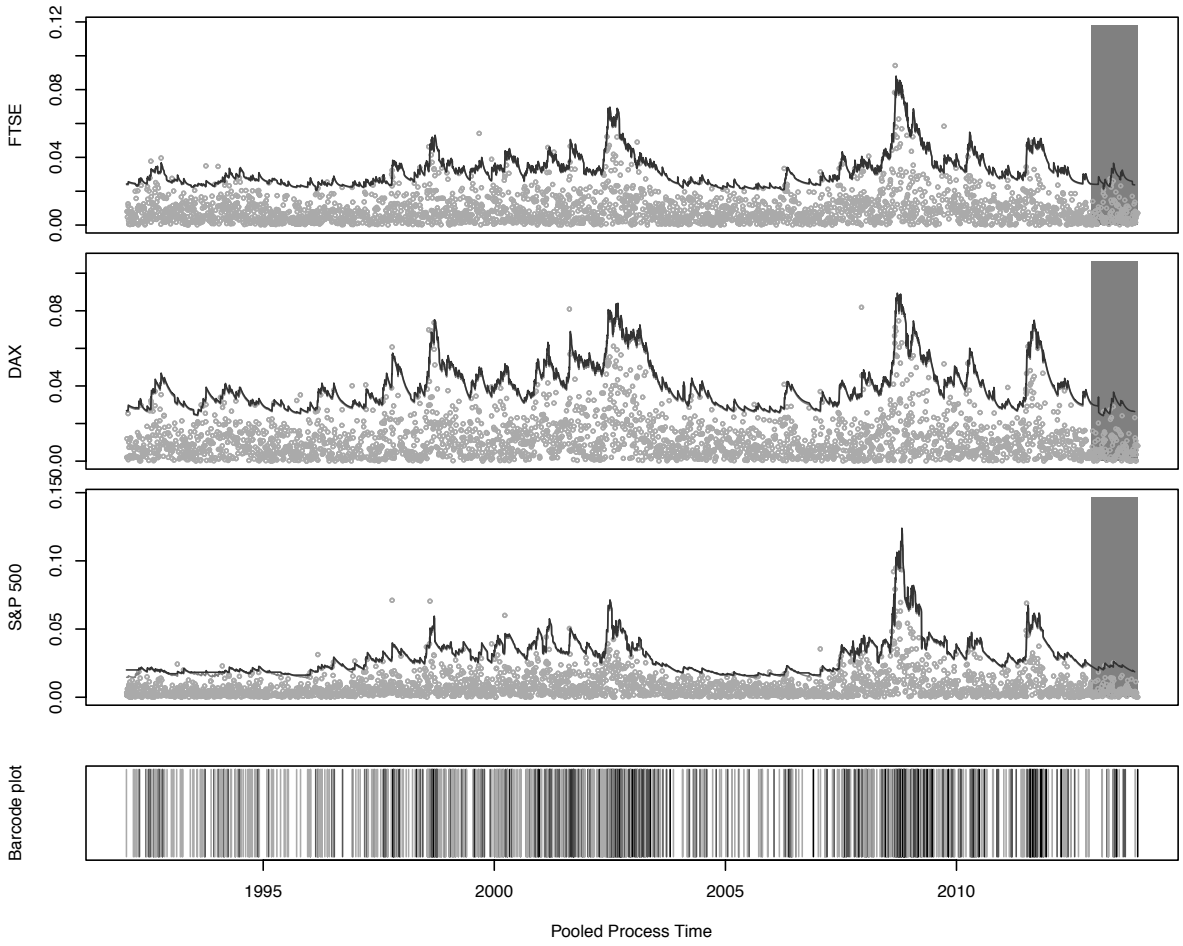

Figure 8: From top to bottom: estimated 99%-VaR (gray line) and 97.5% ES (black line) for the trivariate Hawkes-POT model, applied to the negative log returns of the FTSE 100, DAX and S&P 500 indexes. In-sample period: January 2, 1992 to December 31, 2012. Out-of-sample period: January 2, 2013 to December 31, 2013 (marked by dark background). The bottom panel shows a barcode plot with light colors indicating extreme events in the FTSE 100, DAX, or S&P 500 and the the middle dark colors indicating a simultaneous extreme event in any pair of negative log returns. The dark black color marks a simultaneous extreme event in all three negative log return series.

should be then higher than one. Table 4 reports the time series average (in-sample and backtesting periods) of this ratio for all models and return series. The results indicate that the ratios are nearly identical for both approaches, but are slightly higher in case of the ACI-POT model.

8. Conclusions

We propose a multivariate dynamic intensity model to jointly model the occurrence of extreme observations (exceeding a threshold) in a multivariate time series of log returns. The event arrival is modeled as a marked point process where the marks are associated with the magnitude of (loss) exceedances. The major feature of the model is to allow for clustering of the arrival of extremes over both time and the cross-section and clustering of the size of exceedances. This is achieved by combining a multivariate dynamic intensity process (autoregressive conditional intensity process or Hawkes process) with a multiplicative error model based on a generalized Pareto distribution for the magnitude of exceedances. Both components are linked to allow for feedback effects between the arrival intensity of extremes and the size of exceedances above a threshold.

Empirical evidence based on return series of the DAX, S&P500 and FTSE100 index provides strong support for the model. We find significant evidence for (co-)cluster structures in extreme stock market losses which are well captured by the proposed model. We moreover show that the new model yields a good out-of-sample backtesting performance if it is applied to prediction of Value-at-Risk and Expected Shortfall.

We see it as a major advantage of the proposed framework that it can be easily extended in various directions and – in dependence of the chosen specification – is also tractable in higher dimensions. Consequently, it might be use as a valuable framework to analyze, for instance, systemic risk and to analyze tail dependencies.

References

Artzner, P., Delbaen, F., Eber, J.-M. & Heath, D. (1999), 'Coherent measures of risk', *Mathematical finance* **9**(3), 203–228.

Bacry, E., Dayri, K. & Muzy, J.-F. (2012), 'Non-parametric kernel estimation for symmetric hawkes processes. application to high frequency financial data', *The European Physical Journal B* **85**(5), 1–12.

Bacry, E., Delattre, S., Hoffmann, M. & Muzy, J.-F. (2013), 'Modelling microstructure noise with mutually exciting point processes', *Quantitative Finance* **13**(1), 65–77.

Baltzer, M., Cappiello, L., Santis, R. A. D. & Manganelli, S. (2008), 'Measuring financial integration in new eu members states', *Occasional Papers Series, European Central Bank* **81**.

Baur, D. G., Dimpfl, T. & Jung, R. C. (2012), 'Stock return autocorrelations revisited: A quantile regression approach', *Journal of Empirical Finance* **19**(2), 254–265.

Bauwens, L. & Hautsch, N. (2006), 'Stochastic conditional intensity processes', *Journal of Financial Econometrics* **4**, 450–493.

Bauwens, L. & Hautsch, N. (2009), Modelling financial high frequency data using point processes, *in* J.-P. K. T. G. Andersen, R. A. Davis & T. Mikosch, eds, 'Handbook of Financial Time Series', Vol. 6, Springer, pp. 953–979.

BCBS (2012), 'Fundamental review of the trading book', *Basel Committee on Banking Supervision* .

BCBS (2013), 'Fundamental review of the trading book: A revised market risk framework', *Basel Committee on Banking Supervision* .

Bondt, W. F. & Thaler, R. (1985), 'Does the stock market overreact?', *The Journal of finance* **40**(3), 793–805.

Bondt, W. F. & Thaler, R. (1987), 'Further evidence on investor overreaction and stock market seasonality', *The Journal of Finance* **42**(3), 557–581.

Bowsher, C. G. (2007), 'Modelling security market events in continuous time: Intensity based, multivariate point process models', *Journal of Econometrics* **141**(2), 876–912.

Byström, H. N. (2004), 'Managing extreme risks in tranquil and volatile markets using conditional extreme value theory', *International Review of Financial Analysis* **13**(2), 133–152.

Chang, L.-B., Geman, S., Hsieh, F. & Hwang, C.-R. (2013), 'Invariance in the recurrence of large returns and the validation of models of price dynamics', *Physical Review E* **88**(2), 022116.

Chavez-Demoulin, V., Davison, A. & McNeil, A. (2005), 'A point process approach to value-at-risk estimation', *Quantitative Finance* **5**, 227–234.

Chavez-Demoulin, V., Embrechts, P. & Sardy, S. (2014), 'Extreme-quantile tracking for financial time series', *Journal of Econometrics (to appear)* .

Chavez-Demoulin, V. & McGill, J. (2012), 'High-frequency financial data modeling using hawkes processes', *Journal of Banking & Finance* **36**(12), 3415–3426.

Christoffersen, P. (1998), 'Evaluating interval forecasts', *International economic review* pp. 841–862.

Cotter, J. & Dowd, K. (2006), 'Extreme spectral risk measures: An application to futures clearinghouse margin requirements', *Journal of Banking and Finance* **30**, 3469–3485.

Daley, D. & Vere-Jones, D. (2003), *An Introduction to the Theory of Point Processes*, Springer Series in Statistics.

Dassios, A., Zhao, H. et al. (2011), 'A dynamic contagion process', *Advances in applied probability* **43**(3), 814–846.

Davis, R. A., Mikosch, T. & Cribben, I. (2012), 'Towards estimating extremal serial dependence via the bootstrapped extremogram', *Journal of Econometrics* **170**(1), 142–152.

Davis, R. A., Mikosch, T. et al. (2009), 'The extremogram: a correlogram for extreme events', *Bernoulli* **15**(4), 977–1009.

Davison, A. & Smith, R. (1990), 'Models for exceedances over high thresholds', *Journal of the Royal Statistical Society. Series B (Methodological)* pp. 393–442.

Embrechts, P., Kaufmann, R. & Patie, P. (2005), 'Strategic long-term financial risks: Single risk factors', *Computational Optimization and Applications* **32**(1-2), 61–90.

Embrechts, P., Liniger, T., Lin, L. et al. (2011), 'Multivariate hawkes processes: an application to financial data', *Journal of Applied Probability* **48**, 367–378.

Emmer, S., Kratz, M. & Tasche, D. (2013), 'What is the best risk measure in practice? a comparison of standard measures', *arXiv preprint arXiv:1312.1645* .

Engle, R. (2000), 'The econometrics of ultra-high-frequency data', *Econometrica* **68**(1), 1–22.

Engle, R. (2002), 'New frontiers for arch models', *Journal of Applied Econometrics* **17**(5), 425–446.

Engle, R. & Manganelli, S. (2004), 'Caviar', *Journal of Business and Economic Statistics* **22**(4), 367–381.

Engle, R. & Russell, J. (1998), 'Autoregressive conditional duration: A new model for irregularly spaced transaction data', *Econometrica* **66**, 1127–1162.

Errais, E., Giesecke, K. & Goldberg, L. (2010), 'Affine point processes and portfolio credit risk', *SIAM Journal on Financial Mathematics* **1**(1), 642–665.

Gerhard, F. & Hautsch, N. (2002), 'Volatility estimation on the basis of price intensities', *Journal of Empirical Finance* **9**(1), 57–89.

Gneiting, T. (2011), 'Making and evaluating point forecasts', *Journal of the American Statistical Association* **106**(494), 746–762.

Hall, A. & Hautsch, N. (2007), 'Modelling the buy and sell intensity in a limit order book market', *Journal of Financial Markets* **10**(3), 249–286.

Hall, A., Hautsch, N. & McCulloch, J. (2003), 'Estimating the intensity of buy and sell arrivals in a limit order book market', *New Frontiers in Financial Volatility Modelling, Universita degli Studi di Firenze* pp. 1–35.

Hamidieh, K., Stoev, S. & Michailidis, G. (2009), 'On the estimation of the extremal index based on scaling and resampling', *Journal of Computational and Graphical Statistics* **18**(3), 731–755.

Hammoudeh, S., Santos, P. A. & Al-Hassan, A. (2013), 'Downside risk management and var-based optimal portfolios for precious metals, oil and stocks', *The North American Journal of Economics and Finance* **25**, 318 – 334.

Hautsch, N. (2011), *Econometrics of financial high-frequency data*, Springer.

Hawkes, A. (1971), 'Spectra of some self-exciting and mutually exciting point processes', *Biometrika* **58**, 379–402.

Hawkes, A. G. & Oakes, D. (1974), 'A cluster process representation of a self-exciting process', *Journal of Applied Probability* pp. 493–503.

Herrera, R. (2013), 'Energy risk management through self-exciting marked point process', *Energy Economics* **38**(0), 64 – 76.

Herrera, R. & Eichler, S. (2011), 'Extreme dependence with asymmetric thresholds: Evidence for the european monetary union', *Journal of Banking & Finance* **35**(11), 2916 – 2930.

Herrera, R. & Schipp, B. (2009), Self-exciting extreme value models on stock market crashes, *in* B. Schipp & W. Krämer, eds, 'Statistical Inference, Econometric Analysis and Matrix Algebra', Physica, pp. 209–231.

Herrera, R. & Schipp, B. (2013), 'Value at risk forecasts by extreme value models in a conditional duration framework', *Journal of Empirical Finance* **23**, 33 – 47.

Herrera, R. & Schipp, B. (2014), 'Statistics of extreme events in risk management: The impact of the subprime and global financial crisis on the german stock market', *The North American Journal of Economics and Finance (Accepted)* .

Jondeau, E. & Rockinger, M. (2003), 'Testing for differences in the tails of stock-market returns', *Journal of Empirical Finance* **10**(5), 559 – 581.

Longin, F. & Solnik, B. (2001), 'Extreme correlation of international equity markets', *Journal of Finance* **56**, 649–676.

McNeil, A. & Frey, R. (2000), 'Estimation of tail-related risk measures for heteroscedastic financial time series: an extreme value approach', *Journal of Empirical Finance* **7**, 271–300.

Ogata, Y. (1988), 'Statistical models for earthquake occurrences and residual analysis for point processes', *Journal of the American Statistical Association* **83**, 9–27.

Olmo, J. (2005), 'Testing the existence of clustering in the extreme values', *Documentos de trabajo. Economic series (Universidad Carlos III. Departamento de Economía)* **18**(1).

Pickands, J. (1971), 'The two-dimensional poisson process and extremal processes', *Journal of applied Probability* pp. 745–756.

Poon, S.-H., Rockinger, M. & Tawn, J. (2003), 'Modelling extreme-value dependence in international stock markets', *Statistica Sinica* **14**, 929 – 954.

Poon, S., Rockinger, M. & Tawn, J. (2004), 'Extreme value dependence in financial markets: Diagnostics, models, and financial implications', *Review of Financial Studies* **17**(2), 581.

Prentice, R. L. (1974), 'A log gamma model and its maximum likelihood estimation', *Biometrika* **61**(3), 539–544.

Reiss, R.-D. & Thomas, M. (2007), *Statistical analysis of extreme values: with applications to insurance, finance, hydrology and other fields*, Birkhäuser Basel.

Russell, J. (1999), 'Econometric modeling of multivariate irregularly-spaced high-frequency data', *Manuscript, GSB, University of Chicago* .

Santos, P. A., Alves, I. F. & Hammoudeh, S. (2013), 'High quantiles estimation with quasi-port and dpot: An application to value-at-risk for financial variables', *The North American Journal of Economics and Finance* **26**, 487 – 496.

Santos, P. A. & Alves, M. F. (2012), 'Forecasting value-at-risk with a duration-based POT method', *Mathematics and Computers in Simulation* **94**, 295 – 309.

Smith, R. (1989), 'Extreme value analysis of environmetal time series: An application to trend detection in ground-level ozone', *Statistics Sience* **4**, 367–393.

Stacy, E. W. (1962), 'A generalization of the gamma distribution', *The Annals of Mathematical Statistics* pp. 1187–1192.

Tseng, J.-J. & Li, S.-P. (2011), 'Asset returns and volatility clustering in financial time series', *Physica A: Statistical Mechanics and its Applications* **390**(7), 1300–1314.

A. Figures and Tables

Model	ACI-POT				ACI-POT					Hawkes-POT			
Distribution	(G. gamma)				(Burr)								
Log-return m	gains		losses		gains		losses			gains		losses	
	par	(s.e)	par	(s.e)	par	(s.e)	par	(s.e)		par	(s.e)	par	(s.e)
					Ground process								
a_m	1.085	(0.216)	2.550	(0.345)	0.986	(0.200)	2.576	(0.320)	μ_m	0.007	(0.684)	0.018	(0.352)
b_{1m}	0.499	(0.105)	0.161	(0.085)	0.531	(0.088)	0.166	(0.089)	b_{1m}	0.306	(0.291)	0.537	(0.182)
b_{2m}	0.267	(0.046)	0.652	(0.049)	0.230	(0.038)	0.665	(0.048)	b_{2m}	0.175	(0.866)	0.547	(0.176)
v_{1m}	1.245	(0.105)	2.637	(0.186)	1.646	(0.192)	12.745	(72.714)	a_{1m}	0.009	(0.352)	0.053	(0.204)
σ_{1m}	0.835	(0.103)	1.795	(0.486)	0.464	(0.083)	0.191	(0.036)	a_{2m}	0.001	(2.518)	0.041	(0.246)
v_{1m}	-1.142	(0.289)	-0.986	(0.889)	-1.804	(0.267)	5.408	(87.981)	δ_{1m}	0.001<	(1.1E+05)	20.280	(0.416)
δ_m	2.871	(4.321)	17.402	(5.209)	2.133	(4.364)	16.864	(5.254)	δ_{2m}	0.001<	(1.5E+03)	20.486	(0.429)
	Diagnostics												
LL_1	-2824.992				-2841.732					-2889.962			
Spr	0.796				0.804					0.756			
	Residuals												
Mean (ε_m)	-0.034		0.005		-0.045		0.003			0.187		0.271	
$\tilde{\sigma}_\varepsilon$	0.871		1.076		0.873		1.155			0.591		0.791	
Excess.dis	-1.841		1.185		-1.808		2.502			-4.967		-2.731	
$LB_\varepsilon(5)$	0.000		0.957		0.000		0.993			0.854		0.243	
					Mark process								
w^m					-0.391	(0.208)	-0.647	(0.206)					
ρ_m					0.090	(0.024)	0.084	(0.020)					
β_m					0.820	(0.059)	0.761	(0.053)					
γ_m					-0.003	(0.002)	-0.005	(0.002)					
ξ_m					0.088	(0.046)	0.005	(0.050)					
					Diagnostics								
LL_2					1829.263		1704.919						

Table 1: Estimates of the bivariate MI-POT models used for the analysis of the cluster behavior for extreme events of losses and gains of a portfolio based on the log-returns of the FTSE 100, DAX and S&P 500 indeces from January 2, 1992 to December 31, 2012. Standard errors are in parenthesis. LL_1corresponds to the log-likelihood of the ACI or Hawkes part, while LL_2 to the POT part. The Akaike Information Criterion for the models are AIC-POT (generalized gamma)= -1370, ACI-POT (burr)=-1337, Hawkes-POT =-1240. Spr : Spectral radius of the persistence matrix. Mean (ε_m): mean of residuals, $\tilde{\sigma}_\varepsilon$ standard deviation of the residuals, $LB_\varepsilon(5)$: Ljung-Box statistic, *Excess.dis:* excess dispersion test.

Model			ACI-POT				ACI-POT							Hawkes-POT					
Distribution			(G. gamma)				(Burr)												
Log-return m	FTSE		DAX		S&P500		1		2		3			1		2		3	
	par	(s.e)	par	(s.e)	par	(s.e)	par	(s.e)	par	(s.e)	par	(s.e)		par	(s.e)	par	(s.e)	par	(s.e)
									Ground process										
a_m	0.627	(0.071)	0.568	(0.066)	0.459	(0.075)	0.645	(0.066)	0.602	(0.067)	0.387	(0.047)	μ_m	0.034	(0.203)	0.028	(0.212)	0.012	(0.412)
b_{1m}	25.265	(0.229)	19.435	(0.320)	-0.981	(0.259)	-1.860	(0.262)	-1.349	(0.580)	-0.739	(0.990)	b_{1m}	0.097	(1.049)	0.199	(0.300)	0.251	(0.246)
b_{2m}	-32.097	(0.396)	-24.784	(0.001)	1.014	(0.275)	3.183	(0.515)	2.286	(0.382)	0.706	(0.272)	b_{2m}	0.013	(7.060)	0.248	(0.392)	0.279	(0.298)
b_{3m}	10.864	(0.772)	8.707	(0.122)	0.591	(0.387)	-1.288	(0.955)	-0.568	(0.649)	0.652	(0.478)	b_{3m}	0.050	(1.238)	0.023	(3.013)	0.704	(0.141)
v_{1m}	1.237	(0.058)	1.341	(0.062)	1.224	(0.098)	18.612	(0.317)	24.226	(0.399)	5.693	(0.214)	a_{1m}	0.024	(0.982)	0.040	(0.641)	0.136	(0.305)
σ_{1m}	0.351	(0.042)	0.526	(0.105)	1.998	(0.090)	1.423	(0.060)	1.306	(0.056)	1.710	(0.076)	a_{2m}	0.072	(2.473)	0.034	(0.324)	0.079	(0.479)
v_{1m}	0.001	(0.033)	-0.157	(0.254)	-0.964	(0.232)	0.620	(0.349)	0.554	(0.404)	0.174	(0.249)	a_{3m}	0.091	(0.646)	0.105	(1.261)	0.021	(0.261)
δ_m	18.735	(5.084)	13.512	(4.383)	4.319	(4.095)	19.350	(4.967)	13.499	(4.589)	5.149	(4.205)	δ_{1m}	29.047	(0.992)	0.001<	(6117)	16.719	(0.524)
													δ_{2m}	0.001<	(1.129)	33.751	(0.373)	0.001<	(45393)
													δ_{3m}	32.782	(1.029)	0.001<	(1045)	9.486	(0.979)
	Diagnostics																		
LL_1			-4313.139						-4352.557							-4478.326			
Spr			0.958						0.957							0.745			
	Residuals																		
Mean (ε_m)	0.041		0.145		0.169		-0.006		0.005		-0.002			0.452		0.462		0.223	
$\tilde{\sigma}_\varepsilon$	1.111		0.786		0.708		1.014		0.997		0.953			0.729		0.781		0.909	
Excess.dis	0.409		-0.661		-0.843		0.225		-0.040		-0.695			-3.574		-2.973		-1.321	
$LB_\varepsilon(5)$	0.844		0.736		0.564		0.700		0.747		0.634			0.354		0.751		0.674	
									Mark process										
w^m							-0.392	(0.195)	-0.761	(0.204)	-0.324	(0.191)							
ρ_m							0.047	(0.013)	0.018	(0.021)	0.096	(0.023)							
β_m							0.855	(0.047)	0.792	(0.049)	0.819	(0.058)							
γ_m							-0.004	(0.002)	-0.008	(0.001)	-0.001	(0.001)							
ξ_m							0.009	(0.048)	0.009	(0.041)	0.049	(0.044)							
	Diagnostics																		
LL_2							1783.334		1663.95		1747.058								

Table 2: Estimates of the trivariate MI-POT models applied to the negative log-returns of the FTSE 100, DAX and S&P 500 indeces from January 2, 1992 to December 31, 2012. Standard errors are in parenthesis. LL_1corresponds to the log-likelihood of the ACI or Hawkes part, while LL_2 to the POT part. The Akaike Information Criterion for the models are AIC-POT (generalized gamma)= -1684, ACI-POT (burr)=-1606, Hawkes-POT =-1342. Spr : Spectral radius of the persistence matrix. Mean (ε_m): mean of residuals, $\tilde{\sigma}_\varepsilon$ standard deviation of the residuals, $LB_\varepsilon(5)$: Ljung-Box statistic, *Excess.dis:* excess dispersion test.

		VaR in-sample for the trivariate intensity model																							
		ACI-POT *(Generalized Gamma)*							ACI-POT *(Burr)*							Hawkes-POT									
Stock Index	α	fail.	LRuc	LRind	LRcc	DQ_{hit}	DQ_{VaR}	$V^{ES} \times 10^{-4}$	fail.	LRuc	LRind	LRcc	DQ_{hit}	DQ_{VaR}	$V^{ES} \times 10^{-4}$	fail.	LRuc	LRind	LRcc	DQ_{hit}	DQ_{VaR}	$V^{ES} \times 10^{-4}$			
FTSE	0.975	124	0.65	0.56	0.76	0.57	0.84	1.48	128	0.92	0.15	0.34	0.15	0.35	1.46	117	0.27	0.83	0.54	0.83	0.20	0.76			
	0.98125	88	0.36	0.27	0.36	0.28	0.44	1.26	95	0.85	0.14	0.32	0.14	0.32	1.54	88	0.36	0.27	0.36	0.28	0.35	0.66			
	0.9875	51	0.08	0.01	0.01	0.02	0.05	1.01	57	0.34	0.03	0.06	0.03	0.09	1.28	61	0.65	0.21	0.41	0.21	0.43	1.07			
	0.99	38	0.05	0.03	0.01	0.03	0.10	0.91	38	0.05	0.03	0.01	0.03	0.10	0.45	45	0.34	0.41	0.46	0.41	0.68	0.46			
	0.99375	19	0.01	0.71	0.04	0.71	0.90	-1.19	21	0.03	0.68	0.10	0.68	0.73	-0.88	23	0.08	0.65	0.20	0.65	0.88	-0.53			
DAX	0.975	126	0.78	0.13	0.30	0.13	0.17	2.46	121	0.47	0.03	0.08	0.03	0.08	2.12	122	0.52	0.03	0.09	0.04	0.11	1.73			
	0.98125	89	0.42	0.09	0.17	0.09	0.05	2.22	90	0.48	0.10	0.20	0.10	0.14	2.38	88	0.36	0.00	0.01	0.00	0.02	1.82			
	0.9875	50	0.06	0.10	0.04	0.10	0.10	1.74	49	0.04	0.49	0.10	0.49	0.35	1.54	56	0.27	0.15	0.20	0.15	0.29	1.80			
	0.99	39	0.06	0.30	0.11	0.31	0.16	0.67	40	0.09	0.32	0.15	0.32	0.33	1.93	39	0.06	0.04	0.02	0.04	0.09	1.05			
	0.99375	21	0.03	0.07	0.02	0.08	0.08	0.50	18	0.01	0.05	0.00	0.05	0.04	-1.17	22	0.05	0.08	0.04	0.08	0.09	-0.62			
S&P 500	0.975	115	0.20	0.79	0.43	0.79	0.53	0.68	125	0.72	0.29	0.53	0.29	0.26	1.08	115	0.20	0.17	0.17	0.17	0.39	0.24			
	0.98125	86	0.26	0.65	0.48	0.65	0.35	0.19	86	0.26	0.70	0.49	0.70	0.31	-0.02	91	0.55	0.60	0.73	0.61	0.87	0.74			
	0.9875	57	0.34	0.26	0.33	0.26	0.12	-0.38	64	0.95	0.82	0.97	0.82	0.14	0.09	51	0.08	0.31	0.13	0.32	0.60	-0.94			
	0.99	40	0.09	0.43	0.17	0.43	0.54	-1.51	47	0.51	0.35	0.52	0.36	0.25	-0.64	40	0.09	0.43	0.17	0.43	0.67	-1.55			
	0.99375	27	0.34	0.59	0.55	0.60	0.84	-1.44	29	0.56	0.57	0.71	0.57	0.75	-1.46	22	0.05	0.66	0.14	0.67	0.47	-2.38			

		VaR out-sample for the trivariate intensity model																							
		ACI-POT *(Generalized Gamma)*							ACI-POT *(Burr)*							Hawkes-POT									
Stock Index	α	fail.	LRuc	LRind	LRcc	DQ_{hit}	DQ_{VaR}	$V^{ES} \times 10^{-4}$	fail.	LRuc	LRind	LRcc	DQ_{hit}	DQ_{VaR}	$V^{ES} \times 10^{-4}$	fail.	LRuc	LRind	LRcc	DQ_{hit}	DQ_{VaR}	$V^{ES} \times 10^{-4}$			
FTSE	0.975	6	0.98	0.13	0.31	0.13	0.01	2.13	6	0.98	0.13	0.31	0.13	0.02	2.54	7	0.67	0.18	0.38	0.19	0.20	3.90			
	0.98125	5	0.80	0.08	0.21	0.08	0.02	3.31	5	0.80	0.08	0.21	0.08	0.02	3.79	5	0.80	0.08	0.21	0.08	0.12	4.62			
	0.9875	2	0.55	0.85	0.82	0.85	0.39	3.57	3	0.99	0.78	0.96	0.78	0.52	5.34	1	0.18	0.93	0.41	0.93	0.76	2.84			
	0.99	2	0.80	0.85	0.95	0.85	0.37	5.01	1	0.31	0.93	0.59	0.93	0.24	4.36	1	0.31	0.93	0.59	0.93	0.77	4.48			
	0.99375	0	0.08	1.00	0.22	-	-	-	0	0.08	1.00	0.22	-	-	-	0	0.08	1.00	0.22	-	-	-			
DAX	0.975	6	0.98	0.58	0.86	0.58	0.02	3.95	6	0.98	0.58	0.86	0.58	0.04	4.80	5	0.69	0.64	0.83	0.65	0.07	4.85			
	0.98125	5	0.80	0.64	0.87	0.65	0.01	4.99	4	0.82	0.71	0.91	0.71	0.06	5.50	4	0.82	0.71	0.91	0.71	0.10	6.71			
	0.9875	3	0.99	0.78	0.96	0.78	0.04	6.15	2	0.55	0.85	0.82	0.85	0.03	5.14	0	0.01	1.00	0.05	-	-	-			
	0.99	1	0.31	0.93	0.59	0.93	0.37	4.57	1	0.31	0.93	0.59	0.93	0.49	6.32	0	0.03	1.00	0.09	-	-	-			
	0.99375	0	0.08	1.00	0.22	-	-	-	0	0.08	1.00	0.22	-	-	-	0	0.08	1.00	0.22	-	-	-			
S&P 500	0.975	7	0.67	0.51	0.74	0.52	0.36	3.99	7	0.67	0.51	0.74	0.52	0.26	3.30	5	0.69	0.64	0.83	0.65	0.09	0.06			
	0.98125	3	0.46	0.78	0.73	0.78	0.89	3.87	6	0.48	0.58	0.67	0.58	0.33	4.83	5	0.80	0.64	0.87	0.65	0.10	1.57			
	0.9875	2	0.55	0.85	0.82	0.85	0.86	5.41	3	0.99	0.78	0.96	0.78	0.95	5.76	4	0.57	0.71	0.79	0.71	0.26	3.01			
	0.99	0	0.03	1.00	0.09	-	-	-	1	0.31	0.93	0.59	0.93	0.99	6.39	4	0.34	0.71	0.59	0.71	0.24	4.51			
	0.99375	0	0.08	1.00	0.22	-	-	-	0	0.08	1.00	0.22	-	-	-	2	0.69	0.85	0.91	0.85	0.92	6.02			

Table 3: VaR accuracy test for both MI-POT approaches, for the in-sample period (from January 2, 1992 to December 31, 2012) and the backtesting period (January 2, 2013 to December 31, 2013). Entries in the rows are the significance levels (p-values) of the respective tests, with exception of the confidence level α for the VaR, the measure V^{ES}, and the number of failures (fail.). The cells with values (-) means that the test cannot be estimated.

	ACI-POT (G. gamma)	ACI-POT (Burr)	Hawkes-POT	Theoretical
FTSE	1.017	1.023	1.014	1.001
DAX	1.024	1.023	1.020	1.001
S&P500	1.049	1.067	1.033	1.005

Table 4: Ration between both measures of risk for both approaches ($\overline{ES}_{0.975}/\overline{VaR}_{0.99}$) using the mean of these risk measures for the whole period (in-sample and backtesting periods).